RAL GTPases mediate EGFR/MAPK signalling-driven intestinal stem cell proliferation and tumourigenesis upstream of RAS activation.

Mate Naszai[1,3,4], Yachuan Yu[1,2,3], Alvaro R Fernandez[2,3], Emma Sandilands[2,3], Joel Johansson[2], Jim C Norman[2,3], Owen J Sansom[2,3], David Bryant[2,3], Julia B Cordero[1,3*]

[1] Wolfson Wohl Cancer Research Centre, Glasgow G61 1QH, United Kingdom

[2] Cancer Research UK Beatson Institute, Glasgow G61 1BD, United Kingdom

[3] Institute of Cancer Sciences, University of Glasgow, Glasgow G61 1QH, United Kingdom

[4] Present address: St Peter's College, University of Oxford, Oxford OX1 2DL, United Kingdom

*Correspondence: Julia.Cordero@glasgow.ac.uk

Summary

RAS-like (RAL) GTPases function in Wnt signalling-dependent intestinal stem cell proliferation and regeneration. Whether RAL proteins work as canonical RAS effectors in the intestine, and the mechanisms of how they contribute to tumorigenesis remain unclear. Here, we show that RAL GTPases are necessary and sufficient to activate EGFR/MAPK signalling in the intestine. We identify non-canonical roles of RAL GTPases, not as RAS effectors, but rather by acting upstream of RAS activation via induction of EGFR internalization. Knocking down *Drosophila RalA* from intestinal stem and progenitor cells leads to increased levels of plasma membrane-associated EGFR and decreased MAPK pathway activation. Importantly, in addition to impacting stem cell proliferation and damage-induced intestinal regeneration, this function of RAL GTPases drives EGFR-dependent tumorigenic growth in the intestine and in human mammary epithelium. Altogether, our results reveal previously unrecognised cellular and molecular contexts where RAL GTPases become essential mediators of EGFR-driven tissue homeostasis and malignant growth.

Key words: RAL GTPase; EGFR/MAPK signalling; Intestinal Stem Cells; Regeneration; Cancer

Introduction

The precise spatial and temporal regulation of signalling pathway activity is essential for organ development and adult tissue homeostasis. The latter is particularly important in stem cell maintained self-renewing epithelia, such as that of the gastrointestinal tract (Richardson et al., 2014), where cell loss needs to be counteracted by stem cell proliferation and differentiation while limiting the potential for unwanted overgrowth (Radtke and Clevers, 2005). Progressive loss of control over proliferative pathways either through loss of tumour suppressor genes or oncogene activation are associated with tumour development and progression (Hanahan and Weinberg, 2011).

Regulation of intestinal homeostasis involves the coordinated action of multiple evolutionarily conserved signalling pathways, which relay environmental and niche-derived signals to stem cells to ultimately determine their activity (Gehart and Clevers, 2019; Nászai et al., 2015; Scoville et al., 2008). Increasing understanding of how these pathways are regulated not only provides insight into basic stem cell biology, but also sheds light onto pathological conditions often associated with uncontrolled stem cell proliferation, such as cancer (Biteau et al., 2011; Sell, 2010).

Epidermal growth factor receptor (EGFR, also known as ErbB1 or HER1) is a member of the ErbB family of growth factor receptors, which play essential roles in regulating cell proliferation, differentiation and survival (Citri and Yarden, 2006; Wee and Wang, 2017). In the mammalian intestinal epithelium, EGFR is highly expressed in intestinal stem cells (ISC) and transit amplifying cells (Yang et al., 2017). The EGFR ligand, EGF, is released by Paneth cells and the mesenchyme and is required for the maintenance and proliferation of ISCs (Farin et al., 2012; Sato et al., 2009, 2011). Ectopic activation of EGFR signalling in the intestine through exogenous

sources or genetic overexpression of pathway ligands (Bongers et al., 2012; Kitchen et al., 2005; Marchbank et al., 1995), or deletion of the negative regulator leucine-rich repeats and immunoglobulin-like domains protein 1 (Lrig1) (Powell et al., 2012; Wong et al., 2012), leads to elevated ISC proliferation. On the other hand, loss of EGFR signalling induces quiescence of Lgr5+ ISCs *in vitro* (Basak et al., 2017).

Gene amplification and activating point mutations of EGFR are highly prevalent in cancer (Santarius et al., 2010; Yarden and Pines, 2012). Ectopic EGFR/Ras/MAPK signalling is thought to be an early step in colorectal cancer development (Calcagno et al., 2008). Hyperactivation of the pathway accelerates intestinal tumourigenesis driven by *Adenomatous polyposis coli* loss ($Apc^{min/+}$ mice) (Luo et al., 2009), while a genetic background of partial loss-of-function of EGFR (Roberts et al., 2002) or small molecule inhibitor treatment reduce cancer incidence (Roberts et al., 2002; Torrance et al., 2000).

The *Drosophila* intestinal epithelium shares remarkable homology with its mammalian counterpart. The tissue is maintained by intestinal stem cells (ISCs) that replenish the epithelium through progenitor cells called enteroblasts (EB), which differentiate into either the secretory enteroendocrine (EE) cells or the absorptive enterocytes (EC) (Micchelli and Perrimon, 2006; Ohlstein and Spradling, 2006). Importantly, signalling pathways governing intestinal proliferation and differentiation are highly conserved between fruit flies and mammals (Nászai et al., 2015; Miguel Aliaga et al., 2018). Activation of EGFR/Ras/MAPK within ISCs by niche-derived EGF-like ligands is essential to sustain homeostatic and regenerative proliferation of the adult fly midgut, while constitutive pathway activation in ISCs is sufficient to drive intestinal hyperplasia (Biteau and Jasper, 2011; Buchon et al., 2010; Jiang et al., 2011; Xu et al., 2011).

Regulation of EGFR signalling activity is highly dependent on various modes of receptor trafficking throughout the endocytic pathway. Indeed, abnormal trafficking of receptor tyrosine kinases is linked to cancer (Lanzetti and Di Fiore, 2017; Mosesson et al., 2008). Following internalization through Clathrin-mediated (CME) or Clathrin-independent endocytosis (CIE) (Sorkin and Goh, 2009), EGF ligand/receptor complexes can either be targeted for recycling into the plasma membrane (PM), or ubiquitinated and targeted to late endosomes for lysosomal degradation (Sigismund et al., 2008, 2013). Most recently, autophagy has emerged as an important mechanism implicated in the termination of EGFR/MAPK signalling in the intestine (Zhang et al., 2019). While endocytosis is classically considered as a process to terminate pathway activity (Tomas et al., 2014), significant evidence suggests that receptors retain their ability to relay their signal even after internalisation, hence signalling is not limited to the PM (Sadowski et al., 2009). The relative contribution of PM versus intracellular EGFR to downstream signalling *in vivo* remains unclear (Sousa et al., 2012; Teis et al., 2006).

RAL small GTPases are best recognised for their role as effectors of Ras signalling, which has attracted basic and translational research into their potential in cancer development and progression (Moghadam et al., 2017). We recently identified a novel role of RAL GTPases in the regulation of Wnt signalling activity in ISCs through the regulation of Wnt receptor trafficking into intracellular compartments (Johansson et al., 2019). The relevance of RAL GTPases in intestinal tumorigenesis remained unaddressed as their function in the intestine became redundant upon loss of *Adenomatous polyposis coli*, a key driver of colorectal cancer (Johansson et al., 2019). Furthermore, whether RAL proteins (RALs) can impact intestinal biology

beyond Wnt signalling and whether this occurs through their classical role as Ras effectors is unclear.

Here, using the *Drosophila* intestine and human cell lines we uncover an unexpected, non-canonical role of RAL GTPases in activating EGFR/MAPK signalling, upstream of RAS and through induction of EGFR internalization. Our findings support a positive role of receptor tyrosine kinase internalization in signalling activation *in vivo*. We also identify physiological and pathological settings highly sensitive to the presence of RAL proteins, which may provide ideal platforms for the development of therapeutic approaches geared towards the modulation of RAL function.

Results

RAL GTPases are necessary for EGFR/MAPK signalling activation following damage to the intestinal epithelium

We have previously demonstrated that *RalA,* the single *Ral* gene in *Drosophila*, is required for Wnt signalling activation in the *Drosophila* larval wing disc and adult midgut (Johansson et al., 2019). However, we observed that, adult animals derived from larvae with RNAi driven knockdown of *RalA* (*RalA-RNAi)* in the posterior wing disc compartment, using the *engrailed-gal4* driver (*en>*), showed a significantly more severe wing phenotype than that caused by *wingless* knockdown (*wg-RNAi*) (Figure 1A). This led us to hypothesise that RalA may regulate pathways other than Wnt signalling.

EGFR signalling is also a key determinant of wing tissue patterning (Wang, 2000; Zecca and Struhl, 2002) and ISC proliferation in the adult *Drosophila* midgut (Biteau and Jasper, 2011; Buchon et al., 2010; Jiang et al., 2011; Xu et al., 2011). We found that while RNAi-dependent *EGFR* knockdown gave a similarly modest wing phenotype to that observed upon *wg* knockdown, combined *engrailed-gal4*-driven RNAi knockdown of both *wg* and *EGFR* recapitulated the adult wing phenotype of *en>RalA-RNAi* animals (Figure 1A).

We recently reported that *Drosophila RalA* is required within ISCs to induce midgut regeneration following damage by oral infection with *Erwinia carotovora carotovora 15 (Ecc15)* (Johansson et al., 2019). To achieve a global view of intestinal pathways affected by RalA, we performed a transcriptomic analysis by RNAseq of whole midguts from vehicle treated (Mock) or damaged (*Ecc15* fed) control animals or following *RalA* knockdown in intestinal stem and progenitor cells using the e*scargot-*

gal4 driver (*ISC/EB*>) (Micchelli and Perrimon, 2006). Consistent with its effect on ISC proliferation (Johansson et al., 2019), *RalA* knockdown significantly impaired damage-induced upregulation of cell cycle genes (Figure 1B) in the midgut. Additionally, levels of multiple transcriptional targets of the EGFR/MAPK pathway (Golembo et al., 1996; Hsu et al., 2001; Jin et al., 2015; Meng and Biteau, 2015), such as *argos* (*aos*), *rhomboid* (*rho*), *Sox21a* and *string* (*stg*) were increased following *Ecc15* infection in control midguts. The upregulation of these target genes was significantly impaired upon *RalA* knockdown (Figure 1B). RT-qPCR confirmed RNAseq results (Figure 1C). Furthermore, immunofluorescence staining for the EGFR/MAPK-dependent transcription factor Sox21a (Meng and Biteau, 2015) and the activated form of the MAPK, phosphorylated ERK (pERK), in control animals and following *RalA* knockdown from ISCs/EBs confirmed the need for *RalA* for upregulation of MAPK signalling and downstream targets following damage to the midgut (Figure 1D-G and Figure1—figure supplement 1A-D). Together, these results suggest that *RalA* is necessary for damage-induced EGFR/MAPK activation in the *Drosophila* adult midgut.

Previously, we showed that the role of RAL proteins in Wnt signalling activation and intestinal regeneration is conserved between *Drosophila* and mice (Johansson et al., 2019). The mouse intestine has a robust capacity to regenerate following damage by gamma irradiation, as demonstrated by an increase in the number of regenerating crypts 72 h following irradiation (Cordero et al., 2014; Johansson et al., 2019). We next assessed whether MAPK activation in the regenerating mouse intestine required RAL GTPases. Single conditional knockout of either *Rala* (*Rala*$^{fl/fl}$) or *Ralb* (*Ralb*$^{fl/fl}$) in the murine intestinal epithelium using the *Villin-CreER* driver significantly impaired pERK activation in regenerating intestines when compared to control

(*VillinCre*^{ER}) (Figure 1H). Therefore, RAL GTPases' requirement for EGFR/MAPK pathway activation in the intestinal epithelia is evolutionarily conserved between fruit flies and mammals.

RAL GTPases are sufficient for EGFR/MAPK signalling activation in the *Drosophila* midgut

Ectopic expression of wild-type *RalA* in ISC/EB is sufficient to induce Wnt pathway activation and intestinal proliferation in the *Drosophila* midgut (Johansson et al., 2019). To determine whether RalA is also sufficient to induce EGFR/MAPK signalling, we assessed Sox21a (Figure 1I, J) and pERK (Figure 1K, L) levels by immunostaining following *RalA* overexpression in the midgut . We observed increased levels of both proteins within the ISC/EB compartment compared to the control condition. These results suggest that RAL GTPases are indeed sufficient for EGFR/MAPK pathway activation in the intestinal epithelium.

RALA activation is necessary for ISC proliferation in *Drosophila*

Small GTPases cycle between two alternative conformations: inactive (GDP-bound) and active (GTP-bound). The balance between these states is determined by the activity of guanine nucleotide exchange factors (GEF) and GTPase activating proteins (GAP), which activate and inactivate GTPases, respectively (Neel et al., 2011). There are seven Ral GEFs in the human genome, RALGDS, RALGPS1-2 and RGL1-4, which are often found misregulated in cancer (González-García et al., 2005; Koyama and Kikuchi, 2001; Rodriguez-Viciana and McCormick, 2005) and are considered emerging therapeutic targets (Neel et al., 2011; Vigil et al., 2010). However, the *in vivo* role of RAL GEFs in the intestine remains unknown. Several Ral GEFs are conserved in *Drosophila* (Gentry et al., 2014): Rgl, GEFmeso and CG5522

(*RalGPS*). Rgl is a close orthologue of mammalian RGL (Mirey et al., 2003), GEFmeso was identified in a yeast two hybrid screen using active RalA as bait (Blanke and Jäckle, 2006), while CG5522 was identified based on its close homology to mammalian RalGPS1 (Hu et al., 2011).

We next tested the functional role of each of these RAL GEFs in the fly midgut though RNAi-driven targeted knockdown and assessment of their impact on intestinal regeneration following oral infection with *Ecc15* (Basset et al., 2000). The regenerative capacity of the adult posterior midgut (R4-R5) was quantified as per the number of proliferating ISCs, identified by staining with phosphorylated histone H3 antibody (pH3). As expected, *Ecc15* infection induced significant increase in ISC proliferation relative to mock-treated control animals (Figure 2A-D). Knocking down either of the three RalGEFs of interest significantly impaired regenerative ISC proliferation in the midgut (Figure 2A-D) to levels comparable to those observed upon *RalA* knockdown (Johansson et al., 2019). Furthermore, RalGEF knockdown led to significant reduction in MAPK activation in the midgut following damage (Figure 2E, F). These results provide evidence highlighting the importance maintaining the active status of RALA for robust stem cell proliferation and MAPK activation in the intestine.

RALs regulates EGFR signalling in the intestine upstream of Ras activation

We next assessed how EGFR/MAPK signalling is regulated by RalA in the *Drosophila* midgut. EGFR is overexpressed in ~20% of breast and ~80% of colorectal cancers (Rimawi et al., 2010; Spano et al., 2005), and activating mutations of Ras are one of the most common cancer-associated genetic alterations (Prior et al., 2012). Consistent with previous reports (Jiang et al., 2011; Zhang et al., 2019), activation of the MAPK pathway in the adult *Drosophila* midgut by ISC/EB-specific

overexpression of wild-type EGFR (*EGFR*^{WT}) or constitutively active Ras (*Ras*^{V12}) was sufficient to induce intestinal hyperproliferation (Figure 3A, B). Concomitant downregulation of *RalA* suppressed *EGFR*^{WT}- but not *Ras*^{V12}-driven ISC hyperproliferation (Figure 3A, B and Figure3—figure supplement 1A, B). Consistently, *RalA* knockdown impaired activation of ERK following *EGFR*^{wt} but not *Ras*^{V12} overexpression (Figure 3C, D).

RALA potentiates EGFR signalling activity downstream of ligand binding

Increasing the pool of receptors available for ligand binding, such as through recycling of intracellular receptor towards the plasma membrane or inhibition of receptor degradation, favours activation of receptor tyrosine kinase signalling, including EGFR (von Zastrow and Sorkin, 2007; Zhang et al., 2019). Therefore, one possible mechanism by which RAL proteins may potentiate EGFR signalling in the intestine is by facilitating ligand/receptor interactions. In that case, ligand-independent, constitutively active forms of EGFR, which are linked to cancer (Endres et al., 2014), should be insensitive to RAL deficiency. To test this prediction, we co-expressed *RalA-RNAi* with two active mutant forms of EGFR — *EGFR*$^{\lambda top}$ *and EGFR*^{A887T} — in *Drosophila* intestinal stem and progenitor cells (Figure 3E, F). *EGFR*$^{\lambda top}$ includes an extracellular dimerization domain that causes receptor activation even in the absence of ligand (Queenan et al., 1997), and *EGFR*^{A887T} contains an activating point mutation in the receptor kinase domain (Lesokhin et al., 1999). Overexpression of *EGFR*$^{\lambda top}$ or *EGFR*^{A887T} led to ISC hyperproliferation levels comparable to those observed following *Ras*^{V12} overexpression (Figure 3E, F compare with Figure 3A, B and Figure 3—figure supplement 1A, B). However, unlike in the case of *Ras*^{V12}, knocking down *RalA* significantly impaired *EGFR*$^{\lambda top}$- or *EGFR*^{A887T}-driven ISC proliferation (Figure 3E, F). Consistently, *EGFR*$^{\lambda top}$- or

EGFR^{A887T}-dependent ERK activation was also suppressed by *RalA-RNAi* (Figure 3G, H). These results suggest that *RalA* influences EGFR signalling activity downstream of ligand/receptor binding.

RAL GTPases are required for EGFR internalisation

We next tested whether RAL GTPases may induce EGFR/MAPK signalling through regulation of EGFR cellular localization, similarly to their role on the Wnt receptor Frizzled (Johansson et al., 2019),. Firstly, we used immunostaining to visualise EGFR in control adult *Drosophila* midguts or following genetic manipulation of *RalA* expression. We found that knocking down *RalA* in stem and progenitor cells led to significantly increased levels of PM-associated EGFR (Figure 4A-D). This effect of RalA applied to wild type (Figure 4A, B) and A887T mutant EGFR (Figure 4C, D). Conversely, overexpression of wild-type RalA decreased membrane localisation of EGFR (Figure 4E, F). We were unable to assess the RalA impact on *EGFR*$^{\lambda top}$ localization as our antibody, designed to bind the extracellular domain of EGFR, failed to recognise this mutant version of the receptor. These results strongly suggest that RalA induction of EGFR/MAPK signalling in the intestine involves an increase in the intracellular pool of EGFR.

Next, we used surface biotinylation-based assay to quantify the rate of EGFR internalization in H1299, a human non-small cell lung cancer (NSCLC) cell line with intact EGFR signalling (Amann et al., 2005). To obtain a measure of endocytosis that was not influenced by the rate at which the receptor returns, or ‘recycles’, to the cell surface from endosomes, we performed the surface biotinylation-based assay in the presence of the receptor recycling inhibitor, primaquine. This clearly indicated that EGF-driven (but not EGF-independent) endocytosis of EGFR was significantly reduced by combined knockdown of *Rala* and *Ralb* (Figure 4G and Figure4—figure

supplement 1A, B). By contrast, internalization of integrin α5β1 and transferrin receptor (hTfnR) were not affected by *Rala/b* knockdown (Figure 4—figure supplement 1C, D). These results suggest that the effect of RAL GTPases on EGFR cellular localisation is conserved between *Drosophila* and mammals, and that RAL proteins function in a context-dependent manner, as opposed to being generally required for transmembrane receptor trafficking dynamics.

RAL proteins are necessary for EGFR dependent tumorigenesis

Intestinal hyperplasia caused by hyperactivation of β-Catenin or RAS is independent of RAL proteins (Johansson et al., 2019) (Figure 3A, B). Therefore, the importance of RAL GTPases in intestinal malignancy remains unaddressed. The effect of *Ral* knockdown on intestinal hyperproliferation caused by overexpression of wild type or constitutively active mutants of EGFR in the intestine (Figure 3A-F) suggests that other pathological settings driven by exacerbated EGFR activity might also be sensitive to RAL protein function.

c-Src is a conserved non-receptor tyrosine kinase whose expression is necessary and sufficient to drive regeneration and tumourigenesis of both the *Drosophila* and mouse intestine through EGFR/MAPK activation (Cordero et al., 2014; Kohlmaier et al., 2015) (Figure 5A, B). Consistently, *Src* overexpression in ISCs/EBs (*esg*^{ts}*>Src64*^{wt}) induced expression of the MAPK pathway transcriptional target Sox21a (Figure 5C, D) and pERK levels (Figure 5E, F) (Cordero et al., 2014; Kohlmaier et al., 2015). Importantly, knocking down *RalA* (*ISC/EB>Src64*^{wt}*; RalA-RNAi*) significantly suppressed Src-driven ISC hyperproliferation and MAPK signalling activation in the *Drosophila* midgut (Figure 5A-F). Interestingly, this effect of RalA correlated with an increase in membrane *versus* intracellular levels of EGFR

in *ISC/EB>Src64*^{wt}*; RalA-RNAi* midguts when compared to *ISC/EB>Src64*^{wt} (Figure 5G, H).

As a proof of principle in an orthogonal mammalian system dependent on EGFR for morphogenesis, we employed the human breast tumour cell line HMT3522 T4-2 (henceforth referred to as 'T4-2') as a paradigm to test the role of mammalian RAL GTPases in malignant growth. T4-2 is a subline obtained after spontaneous malignant transformation of the benign breast tumour cell line HMT3522 S1 (henceforth 'S1'). Compared to the S1 predecessor, T4-2 cells grow as disorganised aggregates of cells when cultured in 3Dimensional (3D) Extracellular Matrix gels such as Matrigel. This growth and morphogenesis in 3D in T4-2 cells is EGFR-dependent: T4-2 show robustly upregulated EGFR levels and activation, their growth is independent of exogenous EGF, and they are acutely sensitive to EGFR inhibitors (Madsen et al., 1992; Wang et al., 1998). Thus, we hypothesized that T4-2 growth would be dependent on RAL function.

Consistent with previous reports (Madsen et al., 1992; Wang et al., 1998), treating T4-2 cells with two structurally independent EGFR inhibitors, Tyrphostin (AG1478) and erlotinib, resulted in defective growth as determined by a reduction in 3D acinus size (Figure 5I, J). Importantly, stable depletion of *RalA* or *RalB* in T4-2 by shRNA (Figure 5—figure supplement 1A, B) phenocopied EGFR inhibition, as determined by a significant reduction in 3D acinus size (Figure 5K, L). Therefore, RalA/B function is similarly required for a mammalian morphogenetic function that is dependent on EGFR. Altogether, our results uncover a conserved role of RAL GTPases mediating EGFR/MAPK-dependent tissue homeostasis and transformation upstream of Ras activation.

Discussion

Spatial and temporal regulation of signal transduction by the endocytic pathway plays a key role in health and pathophysiology (Casaletto and McClatchey, 2012; von Zastrow and Sorkin, 2007). The impact of this process in adult stem cells and tissue homeostasis is only recently becoming evident through reports on the effect of endocytosis and autophagy on intestinal stem cell (ISC) proliferation through modulation of Wnt/β-Catenin and EGFR/MAPK activity, respectively (Johansson et al., 2019; Zhang et al., 2019).

In this study, we identify a role for the Ras-related protein RAL in the activation of EGFR/MAPK signalling activity upstream of its known activator RAS through regulation of EGFR internalization. Preventing RAL function in *Drosophila* intestinal stem/progenitor cells reduces the intracellular pool of EGFR, leading to decreased MAPK activation and downstream signalling. This role of RAL proteins impacts stem cell proliferation and regeneration of the intestinal epithelium and has implications in pathological settings that depend on active EGFR signalling, including intestinal hyperplasia and breast cancer cell growth.

RAL GTPases as regulators of signal transduction

While internalization is recognised as the initial means to attenuate signal transduction through reduction of plasma membrane receptors available for activation by extracellular ligands (Goh et al., 2010; Sousa et al., 2012; Vieira et al., 1996; von Zastrow, 2003), the subsequent outcome of endocytosis on signalling is dependent on the trafficking pathway followed by internalised receptors. Internalisation of membrane EGFR through Clathrin-mediated endocytosis (CME) results in prolonged EGFR signalling by favouring receptor recycling back to the plasma membrane, while Clathrin-independent endocytosis (CIE) leads to EGFR

degradation and signalling attenuation (Sigismund et al., 2008). The differential effect of endocytic trafficking on EGFR has therapeutic implications as Clathrin inhibition can divert a tyrosine kinase inhibitor-resistant form of EGFR from CME and recycling to pinocytosis and degradation in non-small cell lung carcinoma (Ménard et al., 2018).

Here, we provide robust evidence of physiological and pathological contexts in the intestine where the internalisation of EGFR mediated by RAL GTPases directly correlates with potentiation of downstream MAPK signalling. We recently reported a similar effect of RAL proteins on seven transmembrane class of receptors Frizzled, leading to high threshold of Wnt signalling activity (Johansson et al., 2019). In both cases, the ultimate outcome of RAL action is an efficient acute proliferative response of intestinal stem cells and tissue regeneration following damage. Therefore, RAL GTPases are effectors of two pivotal signal transduction pathways within the intestinal epithelium (Biteau and Jasper, 2011; Buchon et al., 2010; Jardé et al., 2020; Jiang et al., 2011; Perochon et al., 2018; Sato et al., 2009; Xu et al., 2011). The effect of knocking down *RalA* in the *Drosophila* midgut is, however, milder than that observed upon individual or combined impairment of Wnt/β-Catenin and EGFR/MAPK signalling reception in ISCs (Xu et al., 2011). This suggests that RalA is only partly responsible for the activation of these signalling pathways and its effect is only evident in the regenerative response to damage, which requires high thresholds of signalling activity to allow acute stem cell proliferation for tissue regeneration. The scenario is different in the mammalian intestine, where combined knockout of *Rala* and *Ralb* leads to complete disruption of intestinal epithelial homeostasis (Johansson et al., 2019). This may relate to inherent differences in the signalling activity levels needed to maintain homeostatic ISC proliferation in the fly

midgut versus the mouse intestine. Compared to its murine counterpart, basal proliferation in the adult fly midgut is relatively low and there is no transit amplifying proliferative zone (Micchelli and Perrimon, 2006; Ohlstein and Spradling, 2006).

RAL GTPases have been linked to CME via interaction of their effector protein, RAL binding protein (RALBP1), with the Clathrin adaptor AP2 (Jullien-Flores et al., 2000). More recently, RAL proteins have also been shown to engage in Caveolin-mediated endocytosis (Jiang et al., 2016). While the potentiating effect of RALs on EGFR signalling activity would favour a role of the small GTPases in CME in the system, this needs to be directly assessed. Experiments to functionally connect RalA with specific endocytic trafficking pathways using *Drosophila* genetics have been unsuccessful as, consistent with recently published work (Zhang et al., 2019), global perturbation of the trafficking machinery within ISCs leads to very severe disruption of intestinal homeostasis (data not shown), precluding the establishment of meaningful genetic interactions.

Future research will need to be done to better elucidate the place of action of RAL GTPases within the endocytic trafficking pathway and its connection with EGF and Wnt receptors in the intestine. The use of fluorescently tagged endocytic proteins (Dunst et al., 2015) combined with recently developed live imaging approaches in the adult *Drosophila* intestine (Koyama et al., 2020; Martin et al., 2018) offers a clear opportunity to visualise spatial and temporal receptor/endosome interactions *in vivo*.

RAL GTPases as potential therapeutic targets in cancer

EGFR function is frequently altered in cancer (Santarius et al., 2010; Yarden and Pines, 2012). Excessive protein levels due to gene amplification or increased-transcription are the most common EGFR perturbations found in gastrointestinal and

lung adenocarcinoma as well as in cholangiocarcinoma (Birkman et al., 2016; Jung et al., 2017; Li et al., 2008). On the other hand, EGFR kinase domain activating point mutations are associated with non-small cell lung carcinoma and glioblastoma, but are rarely seen in other types of cancer (Li et al., 2008; Siegelin and Borczuk, 2014; Zhang et al., 2016). Extracellular domain truncating mutations yielding to constitutively active receptor through ligand-independent dimerization have also been observed in glioblastomas (Furnari et al., 2015; Guo et al., 2015; Huang et al., 1997). We have utilised *Drosophila* genetic constructs that mimic all three main classes of EGFR common to human cancers and which lead to intestinal hyperplasia when overexpressed in intestinal stem/progenitor cells (Figure 3). Genetic inhibition of RAL GTPase activity consistently prevented hyperproliferation in these models, suggesting that targeting RAL function could be a potentially effective therapeutic approach in the treatment of multiple highly aggressive cancer types.

Current EGFR-targeted therapies include small molecule tyrosine kinase inhibitors (TKI) and monoclonal antibodies (mAb) against the extracellular domain of the receptor (Xu et al., 2017). A number of resistance mechanisms arise secondary to treatment. Specific kinase domain mutations desensitize cells against TKI (Sequist et al., 2011; Yu et al., 2015), while alterations of the antibody binding site are observed in colorectal cancer (Arena et al., 2015). There is also a tendency for downstream mutations (Raf, Ras, MAPK, MET) to uncouple pathway activity from the receptor (Camidge et al., 2014; Mancini and Yarden, 2016). The most common form of resistance to EGFR-targeted therapies is believed to be innate rather than adaptive (Parseghian et al., 2019). Indeed, about 80% of colorectal cancers are refractive to EGFR therapy (Bardelli and Siena, 2010). Several reports highlight how cancer cells co-opt the endocytic pathway for growth and survival benefits (Mosesson et al.,

2008). In fact, these have been proposed as a potential venue for drug development (Mellman and Yarden, 2013). However, based on the current evidence, we propose that targeting RAL function versus a broader component of the endocytic machinery may prove a more refined approach leading to lower toxic effects (Zhang et al., 2019).

Unexpectedly, our results clearly show that, at least in the intestine, oncogenic mutations in RAS are refractory to RAL GTPase inhibition. Therefore, taking into consideration the genetic composition of the tumour is of outmost importance when considering the use of RAL inhibition as a therapeutic approach.

Materials and Methods

Key resources table

Reagent type (species) or resource	Designation	Source or reference	Identifiers	Additional information
strain, strain background (*Mus musculus*)	VillinCreER	(el Marjou et al., 2004) 10.1002/gene.20042	NA	
strain, strain background (*Mus musculus*)	Ralafl/fl	(Peschard et al., 2012) 10.1016/j.cub.2012.09.013	RRID:MGI:5505291	
strain, strain background (*Mus musculus*)	Ralbfl/fl	(Peschard et al., 2012) 10.1016/j.cub.2012.09.013	RRID:MGI:5505291	
strain, strain background (*Erwinia carotovora carotovora 15*)	Ecc15	B. Lemaitre; (Basset et al., 2000) 10.1073/pnas.97.7.3376	NA	
genetic reagent (*Drosophila melanogaster*)	en>	BDSC	RRID:BDSC_30564	y1 w*; P{w+mW.hs=en2.4-GAL4}e16E
genetic reagent (*Drosophila melanogaster*)	ISC/EB>	S. Hayashi; (Goto and Hayashi, 1999) PMID: 10393119	NA	yw;esg-Gal4NP5130,UAS-GFP,UAS-GFPnLacZ/Cyo;tub-Gal80ts/Tm6B
genetic reagent (*Drosophila melanogaster*)	Control	R. Cagan	NA	w[1118]
genetic reagent (*Drosophila melanogaster*)	RalA-RNAi(1)	VDRC	RRID:FlyBase_FBst0477124	P{KK108989}VIE-260B
genetic reagent (*Drosophila melanogaster*)	RalA-RNAi(2)	BDSC	RRID:BDSC_29580	y1 v1; P{y+t7.7 v+t1.8=TRiP.JF03259}attP2
genetic reagent (*Drosophila melanogaster*)	Wg-RNAi	VDRC	RRID:FlyBase_FBst0476437	P{KK108857}VIE-260B

genetic reagent (*Drosophila melanogaster*)	EGFR-RNAi	VDRC	RRID:FlyBase_FBst0478953	P{KK100051}VIE-260B
genetic reagent (*Drosophila melanogaster*)	RalAwt	G. Hasan; (Richhariya et al., 2017) 10.1038/srep42586	NA	P{UAS-RalA}3
genetic reagent (*Drosophila melanogaster*)	GEFmeso-RNAi	BDSC	RRID:BDSC_42545	y[1] v[1]; P{y[+t7.7] v[+t1.8]=TRiP.HMJ02116}attP40
genetic reagent (*Drosophila melanogaster*)	RalGPS-RNAi	VDRC	RRID:FlyBase_FBst0463650	w[1118]; P{GD11683}v40596/TM3
genetic reagent (*Drosophila melanogaster*)	Rgl-RNAi	BDSC	RRID:BDSC_28938	y[1] v[1]; P{y[+t7.7] v[+t1.8]=TRiP.HM05149}attP2
genetic reagent (*Drosophila melanogaster*)	EGFRwt	BDSC	RRID:BDSC_5368	y[1] w[*]; P{w[+mc]=UAS-Egfr.B}32-26-1
genetic reagent (*Drosophila melanogaster*)	EGFRA887T	BDSC	RRID:BDSC_9533	w[*]; P{w[+mC]=Egfr.2.A887T.UAS}8-2
genetic reagent (*Drosophila melanogaster*)	EGFRλtop	BDSC	RRID:BDSC_59843	w[*]; P{w[+mC]=UAS-Egfr.lambdatop}3/TM6C, Sb[1]
genetic reagent (*Drosophila melanogaster*)	RasV12(1)	BDSC	RRID:BDSC_64195	w[*]; P{w[+mC]=UAS-Ras85D.V12}TL1
genetic reagent (*Drosophila melanogaster*)	RasV12(2)	BDSC	RRID:BDSC_64196	w[*]; P{w[+mC]=UAS-Ras85D.V12}2
genetic reagent (*Drosophila melanogaster*)	Src64wt	BDSC	RRID:BDSC_8477	w[*]; P{w[+mC]=UAS-Src64B.C}2
cell line (*Homo sapiens*)	H1299	ATCC	RRID:CVCL_0060	ATCC CRL-5803
cell line (*Homo sapiens*)	HMT3522 T4-2	V. Weaver, UCSF	RRID:CVCL_2501	

cell line (*Homo sapiens*)	HEK293-FT	Thermo Fisher Scientific	RRID:CVCL_6911	
antibody	GFP	AbCam	RRID:AB_300798	chicken polyclonal anti GFP; 1:2000
	Sox21a	B. Biteau; (Meng and Biteau, 2015) 10.1016/j.celrep.2015.09.061	NA	rabbit polyclonal anti Sox21a; 1:2000
	pERK	Cell Signaling Technology	RRID:AB_331646	rabbit polyclonal anti pERK; 1:100
	pH3	Cell Signaling Technology	RRID:AB_331535	rabbit polyclonal anti Phospho-Histone H3 (Ser10); 1:100
	EGFR (*Drosophila* IHC)	Sigma Aldrich	RRID:AB_609900	mouse monoclonal anti *Drosophila* EGFR extracellular domain; 1:50
	EGFR1 (capture-ELISA)	BDPharmingen	RRID:AB_2096589	mouse anti-EGF Receptor monoclonal
	alpha5 beta1 integrin	BDPharmingen	RRID:AB_396007	Mouse Anti-CD49e Monoclonal Antibody, Unconjugated, Clone VC5
	Transferrin receptor	BDPharmingen	RRID:AB_395918	CD71 human monoclonal antibody
	anti-chicken-IgY-488	Invitrogen	RRID:AB_142924	goat anti-chicken-IgY(H+L)-Alexa Fluor 488
	anti-rabbit-IgG-594	Thermo Fisher Scientific	RRID:AB_2534095	goat anti-rabbit-IgG(H+L)-Alexa Fluor 594
	anti-mouse-IgG-594	Molecular Probes	RRID:AB_141672	goat anti-mouse-IgG(H+L)-Alexa Fluor 594
	pERK (ISH)	Cell Signaling Technology	RRID:AB_331646	rabbit anti-p-ERK1/2 1:400
	Total ERK (ISH)	Cell Signaling Technology	RRID:AB_330744	rabbit anti total-Erk1/2 1:40
recombinant DNA reagent	pLKO.1-puromycin	Moffat et al Cell. 2006 Mar 24. 124(6):1283-98	RRID:Addgene_10878	
	VSVG	Trono lab, unpublished, donated to Addgene	RRID:Addgene_12259	
	SPAX2	Trono lab, unpublished,	RRID:Addgene_12260	

		donated to Addgene		
sequence-based reagent	Rho_Fwd	This paper	NA	TTGTCATCTTTGTCTCCTGCGA
	Rho_Rev	This paper	NA	GTCAGGTGGGCAATGTACGA
	Stg_Fwd	This paper	NA	CAGTAATAACACCAGCAGTTCGAG
	Stg_Rev	This paper	NA	GTAGAACGACAGCTCCTCCT
	Sox21a_Fwd	This paper	NA	AGACAATTAATACAGAGCTCGAGG
	Sox21a_Rev	This paper	NA	GAGATGCTCGTCATGATGCC
	Rpl32_Fwd	This paper	NA	AGGCCCAAGATCGTGAAGAA
	Rpl32_Rev	This paper	NA	TGTGCACCAGGAACTTCTTGAA
	Rala_Fwd	PrimerBank	ID#324072795c2	GCAGACAGCTATCGGAAGAAG
	Rala_Rev	PrimerBank	ID#324072795c2	TCTCTAATTGCAGCGTAGTCCT
	Ralb_Fwd	PrimerBank	ID#48762927c1	AGCCCTGACGCTTCAGTTC
	Ralb_Rev	PrimerBank	ID#48762927c1	AGCGGTGTCCAGAATATCTATCT
	ActB_Fwd	(Liu et al., 2015) 10.1371/journal.pone.0117058	NA	TGACGTGGACATCCGCAAAG
	ActB_Rev	(Liu et al., 2015) 10.1371/journal.pone.0117058	NA	CTGGAAGGTGGACAGCGAGG
	shScr	This paper	NA	CCGCAGGTATGCACGCGT
	shRala	This paper	NA	GGAGGAAGTCCAGATCGATAT
	shRalb	This paper	NA	CAAGGTGTTCTTTGACCTAAT
	siRNA RalA (human)	Dharmacon	ONTARGET plus - Cat# L-009235-00-0005	
	siRNA RalB (human)	Dharmacon	ONTARGET plus - Ca# L-008403-00-0005	
peptide, recombinant protein	EGF	Sigma	Cat# 11376454001	

commercial assay or kit	High Capacity cDNA Reverse Transcription Kit	Applied Biosystems	Cat# 4368813	
	PerfeCTa SYBR Green FastMix (Low ROX)	Quanta Bio	Cat# 95074-012	
	VECTASHIELD Mounting Medium with DAPI	Vector Laboratories, Inc	RRID:AB_2336790	
	RNAeasy Mini Kit (50)	Qiagen	Cat# 74104	
	Growth Factor Reduced Matrigel	BD Biosciences		
	Lipofectamine 2000	Thermo Fisher Scientific	Cat# 11668027	
	Lenti-X Concentrator	Clonetech		
chemical compound, drug	Glutamine	Thermo Fisher Scientific	25030081	
	Insulin	Sigma Aldrich	I0516	Insulin solution from bovine pancreas,10 mg/mL insulin in 25 mm HEPES, pH 8.2, BioReagent, sterile-filtered, suitable for cell culture
	Transferrin	Sigma Aldrich	T2252	
	Sodium selenite	Sigma Aldrich	S5261	
	beta-estradiol	Sigma Aldrich	E2758	
	hydrocortisone	Sigma Aldrich	H0888	
	Prolactin	Miltenyi Biotech	130-093-985	
	Tyrphostin-AG1478	Sigma Aldrich	T4182	
	Erlotinib, HCL	Sigma Aldrich	SML2156	
	puromycin	Thermo Fisher Scientific	A1113803	
	Phalloidin	Invitrogen	A12380,	

			A22287	
	Hoechst		H21486	
software, algorithm	Fiji	NIH		1.51n; https://fiji.sc/
	GraphPad Prism 6	GraphPad	RRID:SCR_002798	
	ZEN 2 lite	ZEISS	RRID:SCR_013672	
	7500 Real-Time PCR Software	Applied Biosystems	RRID:SCR_014596	
	Harmony	PerkinElmer		
	BatchQuantify	(Johansson et al., 2019) 10.1016/j.stem.2019.02.002	NA	https://github.com/emltwc/2018-Cell-Stem-Cell
	EGFR_quant	This paper	NA	https://github.com/emltwc/EGFRProject
other	Axio Observer	ZEISS		
	LSM780 microscope	ZEISS		
	BX51 microscope	Olympus		
	Opera Phenix Z9501	PerkinElmer		
	7500 Fast Real-Time PCR System	Applied Biosystems		
	HiSeq 2000	Illumina		
	ImageLock plate	Essen Biosciences		

Experimental models and organisms

Species used: *Drosophila melanogaster, Mus musculus*

Cell lines used: HMT-3522 T4-2 (human breast cancer derived), NCI-H1299 (human lung cancer derived)

Only mated females were used for *Drosophila* experiments.

Drosophila breeding and maintenance

Flies were maintained in humidity and temperature-controlled incubators with a 12-12-hour light-dark cycle. Crosses were kept at 18°C. F1s of the desired genotype were collected 2-3 days of adult eclosion and aged at 29°C for the time needed to allow for transgene activation. Standard rearing medium used: 10g agar, 15g sucrose, 30g glucose, 15g maize meal, 10g wheat germ, 30g treacle and 10g soya flour per litre of distilled water.

Mouse work

Mouse experiments were performed as described in (Johansson et al., 2019), according to the UK Home Office regulations and designed in accordance with the ARRIVE guidelines. Standard diet and water were given ad libitum, and under non-barrier conditions. The Mice strains used are indicated in the resource table. Tamoxifen (Sigma) IP was used to induce *VilCreER* mice at 80 mg/kg. For regeneration experiments, mice were exposed to γ-irradiation from caesium-137 sources. This delivered γ-irradiation at 0.423 Gy min−1. Mice were sampled 3 days following irradiation damage. The smallest sample size was used that would still give a significant difference in accordance with the 3Rs. No distinction between males and females has been made in the mice experiments. All mice were above 20g of weight before eligible participate in any experiment. Experiments were performed on a C57BL/6 (N=3 or more).

IHC of mouse tissue

IHC staining was performed on 4 μm sections of formalin–fixed paraffin embedded (FFPE) tissues were cut, mounted onto adhesive slides and oven-incubated at 60°C

for 2 hours. Sections were dewaxed for 5 minutes in xylene before rehydrating through decreasing concentrations of alcohol followed by washing with H_2O for 5 minutes. FFPE sections underwent heat–induced epitope retrieval in a pre-treatment module. Sections were heated for 20 minutes at 97°C in Sodium Citrate pH6 retrieval buffer (Thermo, TA-250-PM1X) before cooling to 65°C. Slides were removed and washed in Tris Buffered Saline with Tween (TBT) (Thermo, TA-999-TT). Sections were loaded onto the Dako autostainer link48 platform, washed with TBT then peroxidase blocking solution (Agilent, S2023) applied for 5 minutes. Sections were washed with TBT then appropriate antibody was applied to specific slides. Phospho-p44/42 MAPK (Erk1/2) (Cell Signaling, 9101) was applied at 1/400 dilution and p44/42 MAPK (Erk1/2) (Cell Signaling 9102) was applied at 1/40 dilution for 30 minutes. Sections were then washed again with TBT before application of Rabbit Envision (Agilent, K4003) for 30 minutes before washing with TBT. 3,3' diaminobenzidine (Agilent, K3468) was then applied for 10 minutes before washing in H_2O to terminate the reaction. Finally, slides were counterstained with haematoxylin and dehydrated in increasing concentrations of alcohol, then taken through 3 changes of xylene prior to sealing with glass coverslips using DPX mounting media for microscopy.

Brightfield microscopy

Drosophila wings were mounted onto glass slides (VWR) with 13mm x 0.12mm spacers (Electron Microscopy Science). Images were obtained on the Zeiss Axio Observer system. Images were focus stacked using the ZEN 2 software (Zeiss).

Immunofluorescence of *Drosophila* tissues

Immunofluorescent staining was performed as described in (Johansson et al., 2019). Briefly, tissues were dissected and fixed in 4% paraformaldehyde (PFA, Polysciences Inc) at room temperature for a minimum of 30 min. After fixation, tissues were washed 3 times in PBS + 0.2% Triton X-100 (PBST) for 20 min, followed by overnight incubation at 4°C with primary antibodies in PBST + 0.5% Bovine Serum Albumin (BSA) (PBT). Samples were then washed in PBST 3 times 20 minutes and incubated with secondary antibodies in PBT for 3h at room temperature, followed by washing and mounting.

Midguts stained for pERK included a methanol fixation step between PFA fixation and PBST washing steps of the standard protocol. Following PFA fixation methanol was added dropwise to the solution, with the tissues in it until the volume of the liquid is at least double. Tissues were transferred into 100% methanol for minimum 1 minute. PBS was added to the methanol dropwise after which the samples were subjected to the standard staining protocol.

All samples were mounted onto glass slides (VWR) with 13mm x 0.12mm spacers (Electron Microscopy Science) and Vectashield mounting media containing DAPI (Vector Laboratories, Inc). Confocal images were obtained on a Zeiss LSM 780 and processed in the Zeiss ZEN software.

Antibody concentrations used: anti-GFP (1:2000), anti-pERK (1:100), anti-EGFR (1:50), anti-Sox21a (1:2000), anti-pH3S10 (1:100). Secondary antibodies were used as follows: anti-chicken-IgY-488 (1:200), anti-rabbit-IgG-594 (1:100), anti-mouse-IgG-594 (1:100).

***Drosophila* midgut regeneration assay**

Regeneration assays was performed according to (Neyen et al., 2014). Oral infection was induced using *Erwinia carotovora subsp. carotovora 15* (*Ecc15*) (Basset et al., 2000). Bacteria were grown overnight in LB medium in orbital shaker incubator at 29°C, 200 rpm. The bacterial culture was pelleted (Beckman Coulter JS-4.2 rotor, 10 min @3000rpm ≈ 22547 k-factor) and adjusted to OD600 = 200 followed by mixing with a 5% sucrose solution 1:1. Flies used for regeneration experiments were starved for 2 hours prior to infection to synchronize feeding. Animals were moved into vials containing filter paper (Whatman) soaked into 5% sucrose solution (Mock) or the prepared bacterial solution. Flies were dissected 12-16 hours after infection.

Staining quantification

pERK intensity was quantified in 16-bit z-stack confocal images as the average staining intensity within the GFP positive compartment. Sox21a staining was quantified as the average staining intensity within the DAPI positive compartment using BatchQuantify (Johansson et al., 2019).

EGFR membrane/cytoplasmic staining was quantified using a custom ImageJ macro EGFR_quant (https://github.com/emltwc/EGFRProject).

***Drosophila* RNA extraction, RNA-sequencing and RT-qPCR**

Total RNA from a minimum of 25 midguts was extracted using QIAGEN RNAeasy kit, following manufacturer's instructions, including the on-column DNase digestion step. For RNA-seq RNA integrity score was determined (Agilent technologies, D1000 Screen Tape). Sequencing was performed on the HiSeq 2000 platform (Illumina). For RT-qPCR, RNA was quantified using a NanoDrop 2000c Spectrophotometer. cDNA was synthesized using the High-Capacity cDNA reverse transcription kit (Applied Biosystems), according to the manufacturer's recommendations using a

maximum of 2 µg RNA per 20 µL final volume. Quanta SYBR green Master Mix (Low ROX, Fermentas) was used following manufacturer's instructions. Data were obtained and analyzed using the Applied Biosystems 7500 software. Results represent biological quadruplicates ± SEM. Expression of target genes was measured and normalized to *rpl32* using standard curves.

Cell culture

HMT-3522 T4-2 (V. Weaver, UCSF) cells were cultured in precoated collagen plates using DMEM / Ham's F12 (1:1) media supplemented with 2mM Glutamine (Life Technologies), 250ng/ml insulin solution from bovine pancreas (Sigma-Aldrich), 10 µg/ml transferrin (Sigma-Aldrich), 2.6 ng/mL Sodium selenite (Sigma-Aldrich), 10^{-10}M 17 beta-estradiol (Sigma-Aldrich), 1.4 x 10^{-6}M hydrocortisone (Sigma-Aldrich), and 10 ng/ml human prolactin (Miltenyi Biotec).

Culture of cell lines as 3D acini was adapted from David Bryant's protocols. Briefly, single cell suspensions (1.5 x 10^4 cells per ml) were plated in the appropriate medium supplemented with 2% Growth Factor Reduced Matrigel (GFRM; BD Biosciences). 100µl of this mix were added per well in a 96 well ImageLock plate (Essen Biosciences) precoated with 10µl of pure GFRM for 15 minutes at 37 ºC. Cells were incubated at 37 ºC for 5 days, changing the media every two days, before IF.

For inhibitor studies, cells were treated from the time of plating with Tyrphostin-AG1478 (80 nM in ethanol, Sigma-Aldrich), Erlotinib (100 nM in DMSO), and Ethanol or DMSO as appropriate controls, respectively.

HEK293-FT (Thermo Fisher Scientific) were cultured in DMEM supplemented with 10% FBS, 6mM L-glutamine and 0.1mM Non-Essential Amino Acids (NEAA) (all reagents from Life Technologies).

Generation of stable cell lines

Stable cell lines were performed by co-transfecting pLKO.1-puromycin shRNA plasmid with VSVG and SPAX2 lentiviral packaging vectors using Lipofectamine 2000 into HEK293-FT packaging cells according to manufacturer's instructions (Invitrogen). Viral supernatants were collected; filtered using PES 0.45µm syringe filters (Starlab),and concentrated using Lenti-X Concentrator (Clontech) as per the manufacturer's instructions. Cells were then transduced with the lentivirus for 3 days before selection with 1µg/ml puromycin (Thermo Fisher Scientific). shRNA target sequences: shScr (5'CCGCAGGTATGCACGCGT3'), shRalA (5'GGAGGAAGTCCAGATCGATAT3'), and shRalB (5' CAAGGTGTTCTTTGACCTAAT3'). To knockdown RAL protein expression in H1229 cells, cells were transfected with Dharmacon ON-TARGETplus siRNAs using the Amaxa Nucleofector system (Lonza).

RNA extraction and RT-qPCR

RT-qPCR on human samples was performed following the same protocol used for *Drosophila* samples, except using human β-actin or GAPDH to normalize transcript levels using the delta-delta-C_T method.

Cyst growth assay

Acini labelling was adapted from previously described protocols. Briefly, cultures were fixed in 4% paraformaldehyde (PFA, Affimetrix) for 10 min at room temperature (RT), washed twice in PBS, blocked for 1 h in PFS buffer (PBS, 0.7% w/v fish skin

gelatin (Sigma-Aldrich), 0.5% saponin (Sigma-Aldrich), and incubated with primary antibodies diluted in PFS at 4 °C overnight with gentle rocking. Then, cyst cultures were washed three times with PFS and incubated with secondary antibodies diluted in PFS for 1h at RT, followed by washing twice in PFS and twice in PBS. Labelling was performed using Phalloidin (1:200) (Invitrogen) and Hoescht to label nuclei (10 µg ml^{-1}).

Acquisition of confocal images was performed using Opera Phenix Z9501 high-content imaging system (PerkinElmer), imaging at least 10 optical sections every 2 µM, imaging 25 fields at 20x. Images were analysed using Harmony imaging analysis software (PerkinElmer).

Internalisation assay

Internalisation assays were performed as described in (Roberts et al., 2001). Briefly, cells were surface labelled at 4°C with 0.13 mg/ml NHS-SS-biotin (Pierce) in PBS for 30 min. Following surface labelling, cells were transferred to complete medium at 37°C to allow internalization in the presence of 0.6mM primaquine for the indicated times. Biotin was then removed from the cell surface by treatment with the cell-impermeable reducing agent MesNa. Cells were then lysed and the quantity of biotinylated receptors determined using a capture-ELISA. The following antibodies were used for capture-ELISA; clone VC5 (BDPharmingen, Cat 555651) for α5β1, anti-CD71 (BDPharmingen, Cat 555534) for the TfnR and anti-EGFR1 (BDPharmingen, Cat 555996).

Statistical analysis

GraphPad Prism 6 software was used for statistical analyses. Information on sample size, and statistical tests used for each experiment are indicated in the figure legends.

Data availability

All data underlying the findings of this paper will be available at the time of publication through local repositories accessible via a DOI. Custom scripts used for quantification are available at (https://github.com/emltwc). Requests for further information, reagents and resources should be directed to and will be fulfilled by Julia B. Cordero (julia.cordero@glasgow.ac.uk).

Author contributions

M.N. performed and analysed most experiments; Y.Y. provided technical assistance throughout the study; A.R.F and E.S. performed the 3D mammary tumour cell growth assays; J.J., performed the mouse intestinal regeneration experiment; J.C.N. designed, performed and analysed the EGFR internalization experiments; D.B. designed and supervised 3D mammary tumour cell growth assays; O.J.S. design and supervised the mouse intestinal experiments; JBC conceptualized the study, designed the experiments with M.N., supervised the work and analyse the data. M.N. and J.B.C. wrote the manuscript with contributions from J.C.N., O.J.S. and D.B.

Acknowledgements

We would like to thank Björn Kruspig, Sergi Martha Maria Zarou, Gaiti Hasan, Valerie Weaver and Benoit Biteau for reagents. We thank the Vienna Drosophila RNAi Center, the Bloomington Drosophila Stock Center, and the Developmental

Studies Hybridoma Bank for providing *Drosophila* lines and reagents. M.N. was supported by a Leadership Fellowship from the University of Glasgow to (J.B.C.). Y.Y. is supported by CRUK core funding (A17196). The work from the Norman laboratory was funded by Cancer Research UK (CRUK), and J.C.N acknowledges the CRUK Glasgow Centre (C596/A18076). O.J.S is funded by CRUK Core A21139. B.D. and A.R.F are supported by a University of Glasgow and CRUK core funding (CRUK C596/A17196). J.B.C. is a Sir Henry Dale Fellow jointly funded by the Wellcome Trust and the Royal Society (Grant number 104103/Z/14/Z).

Conflicts of interest

O.J.S. has received funding from Novartis to examine RAL and RAL GEFS in malignancy.

Figure legends

Figure 1. Ral GTPases are necessary and sufficient to induce EGFR/MAPK signalling in intestinal stem cells.

A. Adult *Drosophila* wings with posterior compartment knockdown of *wg* (*wg-RNAi*), *Egfr* (*Egfr-RNAi*) or *RalA* (*RalA-RNAi(1)*) or combined *wg* and *Egfr* knockdown (*wg-RNAi* +*Egfr-RNAi*). Scale bar = 500 µm
B. Heat map from transcriptomic analysis of adult whole midguts from mock treated and *Ecc15* infected control animals (+) or following knockdown of *RalA* (*RalA-RNAi(1)*) using the *escargot-gal4, UAS-gfp* driver (ISC/EB>).
C. RT-qPCR confirmation of transcriptional targets of EGFR/MAPK signalling in whole midguts from genotypes and conditions as in B. n=4, Two-way ANOVA followed by Sidak's multiple comparisons test.

D. Representative confocal images of Sox21a immunofluorescence staining (red/grey) of adult posterior midguts from Mock treated or *Ecc15* infected control animals or following knockdown of *RalA* (*RalA-RNAi(1)*) in stem/progenitor cells using *escargot-gal4, UAS-gfp* (ISC/EB>; green).

E. Quantification of average Sox21a staining intensity, within the nuclear compartment (DAPI positive) in midguts as in D. Two-way ANOVA followed by Sidak's multiple comparisons test; each dot represents a z-stack confocal image from independent posterior midguts.

F. Representative confocal images of pERK immunofluorescence staining (red/grey) of adult posterior midguts from Mock treated or *Ecc15* infected control animals or following knockdown of *RalA* (*RalA-RNAi(1)*) within stem/progenitor cells (ISC/EB>; green).

G. Quantification of average pERK staining intensity within the ISC/EB compartment (GFP positive) of midguts as in F. Two-way ANOVA followed by Sidak's multiple comparisons test; each dot represents a z-stack confocal image from independent posterior midguts.

H. Representative immunohistochemistry images of total (bottom panels) and pERK (top panels) in small intestinal regenerating crypts 3 days after whole body irradiation of control mice (left panels) or mice following conditional intestinal epithelial knockout of *Rala* or *Ralb*.

I. Representative confocal images of Sox21a immunofluorescence staining (red/grey) of adult posterior midguts from control animals or animals overexpressing wild-type *Rala* within stem/progenitor cells (ISC/EB>; green).

J. Quantification of average Sox21a staining intensity, within the nuclear compartment (DAPI positive) of midguts as in J. Student's t-test; each dot represents a z-stack confocal image from independent posterior midguts.

K. Representative confocal images of pERK immunofluorescence staining (red/grey) in control animals or animals overexpressing wild-type *Rala* within stem/progenitor cells (ISC/EB>; green).

L. Quantification of average pERK staining intensity, within the ISC/EB compartment (GFP positive) of midguts as in L. Student's t-test; each dot represents a z-stack confocal image from independent posterior midguts.

Where indicated: *$*p<0.05$, $**p<0.01$, $***p<0.001$, $****p<0.0001$.*

Figure 1—figure supplement 1. Ral GTPases are necessary and sufficient to induce EGFR/MAPK signalling in intestinal stem cells.

A. Representative confocal images of Sox21a immunofluorescence staining (red/grey) of adult posterior midguts from Mock treated or *Ecc15* infected control animals or following knockdown of *RalA* (*RalA-RNAi(2)*) in stem/progenitor cells using *escargot-gal4, UAS-gfp* (ISC/EB>; green).

B. Quantification of average Sox21a staining intensity, within the nuclear compartment (DAPI positive) in midguts as in A. Two-way ANOVA followed by Sidak's multiple comparisons test; each dot represents a z-stack confocal image from independent posterior midguts.

C. Representative confocal images of pERK immunofluorescence staining (red/grey) of adult posterior midguts from Mock treated or *Ecc15* infected control animals or following knockdown of *RalA* (*RalA-RNAi(2)*) within stem/progenitor cells (ISC/EB>; green).

D. Quantification of average pERK staining intensity within the ISC/EB compartment (GFP positive) of midguts as in C. Two-way ANOVA followed by Sidak's multiple comparisons test; each dot represents a z-stack confocal image from independent posterior midguts.

Where indicated: *$p<0.05$, **$p<0.01$, ***$p<0.001$, ****$p<0.0001$.

Figure 2. Ral GTPase activation is necessary for EGFR/MAPK signalling in regenerating ISCs/EBs.

A. Representative confocal images of pH3 staining (red) within the ISC/EB compartment (green) in mock-treated or regenerating posterior midguts.

B. Quantification of pH3 positive nuclei in Control or *GEFmeso-RNAi* posterior midguts as in A. Two-way ANOVA followed by Sidak's multiple comparisons test.

C. Quantification of pH3 positive nuclei in Control or *RalGPS-RNAi* posterior midguts as in A. Two-way ANOVA followed by Sidak's multiple comparisons test.

D. Quantification of pH3 positive nuclei in Control or *Rgl-RNAi* posterior midguts as in A. Two-way ANOVA followed by Sidak's multiple comparisons test.

E. Representative confocal images of pERK staining (red/grey) in mock-treated or regenerating Control animals or animals with knockdown of *GEFmeso, RalGPS* or *Rgl* within the ISC/EB compartment (green).

F. Quantification of average pERK staining intensity within the ISC/EB compartment (GFP positive) as in E. Two-way ANOVA followed by Sidak's multiple comparisons test; each dot represents a z-stack confocal image from independent posterior midguts.

Where indicated: *$p<0.05$, **$p<0.01$, ***$p<0.001$, ****$p<0.0001$.

Figure 3. Ral GTPases are required for EGFR/MAPK signalling upstream of Ras.

A. Representative confocal images of pH3 staining (red) within the ISC/EB compartment (green) in Control and wild-type *Egfr* (*EGFR*^{WT}) or constitutive *Ras* (*Ras*^{V12}*(2)*) overexpressing posterior midguts with or without *RalA* knock-down.

B. Quantification of pH3 positive nuclei in posterior midguts, as in A. Two-way ANOVA followed by Sidak's multiple comparisons test.

C. Representative confocal images of pERK staining (red/grey) within the ISC/EB compartment (green) in Control and wild-type *Egfr* (*EGFR*^{WT}) or constitutive *Ras* (*Ras*^{V12}*(2)*) overexpressing posterior midguts with or without *Rala* knock-down.

D. Quantification of average pERK staining intensity, as seen in (C), within the ISC/EB compartment (GFP positive). Two-way ANOVA followed by Sidak's multiple comparisons test; each dot represents a z-stack confocal image from independent posterior midguts.

E. Representative confocal images of pH3 staining (red) within the ISC/EB compartment (green) in Control and two constitutively active *Egfr* constructs (*EGFR*$^{\lambda top}$ or *EGFR*^{A887T}) overexpressing posterior midguts with or without *RalA* knock-down.

F. Quantification of pH3 positive nuclei in posterior midguts, as in E. Two-way ANOVA followed by Sidak's multiple comparisons test.

G. Representative confocal images of pERK staining (red/grey) within the ISC/EB compartment (green) in Control and two constitutively active *Egfr*

constructs (*EGFR*$^{\lambda top}$ or *EGFR*^{A887T}) overexpressing posterior midguts with or without *RalA* knock-down.

H. Quantification of average pERK staining intensity, as in G, within the ISC/EB compartment (GFP positive). Two-way ANOVA followed by Sidak's multiple comparisons test; each dot represents a z-stack confocal image from independent posterior midguts.

Where indicated: *$*p<0.05$, $**p<0.01$, $***p<0.001$, $****p<0.0001$.*

Figure 3—figure supplement 1. Ral GTPases are required for EGFR/MAPK signalling upstream of Ras.

A. Representative confocal images of pH3 staining (red) within the ISC/EB compartment (green) in Control and constitutive *Ras* (*Ras*^{V12}*(1)*) overexpressing posterior midguts with or without *RalA* knock-down (*RalA-RNAi(2)*).

B. Quantification of pH3 positive nuclei in posterior midguts, as in A. Student's t-test.

Figure 4. Ral GTPases are required for EGFR internalisation.

A. Representative images of wild-type EGFR staining in *Drosophila* intestinal epithelium with or without *RalA* knock-down (*RalA-RNAi*). Scale bar = 5 µm

B. Quantification of EGFR plasma membrane staining localisation as in A, relative to the cytoplasm. Student's t-test

C. Representative images of EGFR^{A887T} staining in *Drosophila* intestinal epithelium with or without *RalA* knock-down (*RalA-RNAi*). Scale bar = 5 µm

D. Quantification of EGFR^{A887T} plasma membrane staining localisation as in C, relative to the cytoplasm. Student's t-test

E. Representative images of EGFR staining in *Drosophila* intestinal epithelium with or without wild-type *RalA* over-expression (*RalAwt*). Scale bar = 5 µm

F. Quantification of EGFR plasma membrane staining localisation as in E relative to the cytoplasm. Student's t-test

G. Internalisation of EGFR over time as determined by a surface biotinylation ELISA based assay with or without EGF ligand in wild-type (*Control*) and concomitant *Rala* and *Ralb* knock-down (si*RalA+B*) H1299 human non-small cell lung cancer cells.

Where indicated: **p<0.05, **p<0.01, ***p<0.001, ****p<0.0001.*

Figure 4—figure supplement 1. Ral GTPases are required for EGFR internalisation.

A. Confirmation of knock-down of *Rala* in wild-type (*Control*) and concomitant *Rala* and *Ralb* knock-down (si*RalA+B*) H1299 human non-small cell lung cancer cells.

B. Confirmation of knock-down of *Ralb* in wild-type (*Control*) and concomitant *Rala* and *Ralb* knock-down (si*RalA+B*) H1299 human non-small cell lung cancer cells.

C. Internalisation of α5β1 integrin over time as determined by a surface biotinylation ELISA based assay with or without EGF ligand in wild-type (*Control*) and concomitant *Rala* and *Ralb* knock-down (si*RalA+B*) H1299 human non-small cell lung cancer cells.

D. Internalisation of human transferrin receptor (hTfnR) over time as determined by a surface biotinylation ELISA based assay with or without EGF ligand in wild-type (*Control*) and concomitant *Rala* and *Ralb* knock-down (si*RalA+B*) H1299 human non-small cell lung cancer cells.

Where indicated: *$p<0.05$, **$p<0.01$, ***$p<0.001$, ****$p<0.0001$.

Figure 5. Ral GTPases mediate malignant transformation of the intestinal and mammary epithelium.

A. Representative confocal images of pH3 staining (red/grey) within the ISC/EB compartment (green) in *Src*-kinase (*Src64wt*) overexpressing posterior midguts with or without *Rala* knock-down. White arrows indicate pH3 positive nuclei.
B. Quantification of pH3 positive nuclei in posterior midguts as in A. Student's t-test.
C. Representative confocal images of Sox21a staining (red/grey) within the ISC/EB compartment (green) in *Src*-kinase (*Src64wt*) overexpressing posterior midguts with or without *Rala* knock-down.
D. Quantification of average Sox21a staining intensity within the nuclear compartment (DAPI positive) as in C. Two-way ANOVA followed by Sidak's multiple comparisons test; each dot represents a z-stack confocal image from independent posterior midguts.
E. Representative confocal images of pERK staining (red/grey) within the ISC/EB compartment (green) in *Src*-kinase (*Src64wt*) overexpressing posterior midguts with or without *Rala* knock-down.
F. Quantification of average pERK staining intensity within the ISC/EB compartment (GFP positive) as in E. Two-way ANOVA followed by Sidak's multiple comparisons test; each dot represents a z-stack confocal image from independent posterior midguts.

G. Representative images of EGFR staining in *Src64* over-expressing *Drosophila* intestinal epithelium with or without *Rala* knock-down (*RalA-RNAi*). Scale bar = 5 µm

H. Quantification of EGFR plasma membrane staining localisation relative to the cytoplasm as in G. Student's t-test

I. Confocal fluorescence microscopy images of HMT3522 T4-2 3D cultures, treated with EGFR inhibitors (tyrphostin AG1478 and erlotinib) or corresponding controls (ethanol and DMSO, respectively) followed by fixation after 5 days and stained for F-actin (yellow) and nuclei (blue, Hoechst).

J. Quantification of area of 5-days T4-2 cysts treated as in J. n ≥ 1214 cysts assessed from four wells/condition/experiment, two independent experiments. One-way ANOVA, Tukey's multiple comparisons test.

K. Confocal fluorescence microscopy images of HMT3522 T4-2 cysts of 5-days expressing either scramble, RalA or RalB shRNA. Cysts were fixed and stained for F-actin (yellow) and nuclei (blue, Hoechst).

L. Quantification of 5-days T4-2 cysts treated with the above described conditions. n ≥ 468 cysts assessed from four wells/condition/experiment, three independent experiments. One-way ANOVA, Tukey's multiple comparisons test.

Where indicated: *$p<0.05$, **$p<0.01$, ***$p<0.001$, ****$p<0.0001$.

Figure 5—figure supplement 1. *Ral* knockdown in human mammary cell lines.

A. Confirmation of knock-down of *Rala* in HMT3522 T4-2 3D cultures in the parental, shScr, shRalA and shRalB conditions.

B. Confirmation of knock-down of *Ralb* in HMT3522 T4-2 3D cultures in the parental, shScr, shRalA and shRalB conditions.

Where indicated: *$p<0.05$, **$p<0.01$, ***$p<0.001$, ****$p<0.0001$.

References

Amann, J., Kalyankrishna, S., Massion, P.P., Ohm, J.E., Girard, L., Shigematsu, H., Peyton, M., Juroske, D., Huang, Y., Stuart Salmon, J., et al. (2005). Aberrant epidermal growth factor receptor signaling and enhanced sensitivity to EGFR inhibitors in lung cancer. Cancer Res. *65*, 226–235.

Arena, S., Bellosillo, B., Siravegna, G., Martinez, A., Canadas, I., Lazzari, L., Ferruz, N., Russo, M., Misale, S., Gonzalez, I., et al. (2015). Emergence of Multiple EGFR Extracellular Mutations during Cetuximab Treatment in Colorectal Cancer. Clin. Cancer Res. *21*, 2157–2166.

Bardelli, A., and Siena, S. (2010). Molecular Mechanisms of Resistance to Cetuximab and Panitumumab in Colorectal Cancer. J. Clin. Oncol. *28*, 1254–1261.

Basak, O., Beumer, J., Wiebrands, K., Seno, H., van Oudenaarden, A., and Clevers, H. (2017). Induced Quiescence of Lgr5+ Stem Cells in Intestinal Organoids Enables Differentiation of Hormone-Producing Enteroendocrine Cells. Cell Stem Cell *20*, 177-190.e4.

Basset, a, Khush, R.S., Braun, a, Gardan, L., Boccard, F., Hoffmann, J. a, and Lemaitre, B. (2000). The phytopathogenic bacteria Erwinia carotovora infects

Drosophila and activates an immune response. Proc. Natl. Acad. Sci. U. S. A. *97*, 3376–3381.

Birkman, E.-M., Ålgars, A., Lintunen, M., Ristamäki, R., Sundström, J., and Carpén, O. (2016). EGFR gene amplification is relatively common and associates with outcome in intestinal adenocarcinoma of the stomach, gastro-oesophageal junction and distal oesophagus. BMC Cancer *16*, 406.

Biteau, B., and Jasper, H. (2011). EGF signaling regulates the proliferation of intestinal stem cells in Drosophila. Development *138*, 1045–1055.

Biteau, B., Hochmuth, C.E., and Jasper, H. (2011). Maintaining tissue homeostasis: dynamic control of somatic stem cell activity. Cell Stem Cell *9*, 402–411.

Blanke, S., and Jäckle, H. (2006). Novel guanine nucleotide exchange factor GEFmeso of Drosophila melanogaster interacts with Ral and Rho GTPase Cdc42. FASEB J. *20*, 683–691.

Bongers, G., Muniz, L.R., Pacer, M.E., Iuga, A.C., Thirunarayanan, N., Slinger, E., Smit, M.J., Reddy, E.P., Mayer, L., Furtado, G.C., et al. (2012). A role for the epidermal growth factor receptor signaling in development of intestinal serrated polyps in mice and humans. Gastroenterology *143*, 730–740.

Buchon, N., Broderick, N.A., Kuraishi, T., and Lemaitre, B. (2010). Drosophila EGFR pathway coordinates stem cell proliferation and gut remodeling following infection. BMC Biol. *8*, 152.

Calcagno, S.R., Li, S., Colon, M., Kreinest, P.A., Thompson, E.A., Fields, A.P., and Murray, N.R. (2008). Oncogenic K-ras promotes early carcinogenesis in the mouse proximal colon. Int. J. Cancer *122*, 2462–2470.

Camidge, D.R., Pao, W., and Sequist, L. V. (2014). Acquired resistance to TKIs in solid tumours: learning from lung cancer. Nat. Rev. Clin. Oncol. *11*, 473–481.

Casaletto, J.B., and McClatchey, A.I. (2012). Spatial regulation of receptor tyrosine kinases in development and cancer. Nat. Rev. Cancer *12*, 387–400.

Citri, A., and Yarden, Y. (2006). EGF-ERBB signalling: towards the systems level. Nat. Rev. Mol. Cell Biol. *7*, 505–516.

Cordero, J.B., Ridgway, R.A., Valeri, N., Nixon, C., Frame, M.C., Muller, W.J., Vidal, M., and Sansom, O.J. (2014). c-Src drives intestinal regeneration and transformation. EMBO J. *33*, 1474–1491.

Dunst, S., Kazimiers, T., von Zadow, F., Jambor, H., Sagner, A., Brankatschk, B., Mahmoud, A., Spannl, S., Tomancak, P., Eaton, S., et al. (2015). Endogenously Tagged Rab Proteins: A Resource to Study Membrane Trafficking in Drosophila. Dev. Cell *33*, 351–365.

Endres, N.F., Barros, T., Cantor, A.J., and Kuriyan, J. (2014). Emerging concepts in the regulation of the EGF receptor and other receptor tyrosine kinases. Trends Biochem. Sci. *39*, 437–446.

Farin, H.F., Van Es, J.H., and Clevers, H. (2012). Redundant Sources of Wnt Regulate Intestinal Stem Cells and Promote Formation of Paneth Cells. Gastroenterology *143*, 1518-1529.e7.

Furnari, F.B., Cloughesy, T.F., Cavenee, W.K., and Mischel, P.S. (2015). Heterogeneity of epidermal growth factor receptor signalling networks in glioblastoma. Nat. Rev. Cancer *15*, 302–310.

Gehart, H., and Clevers, H. (2019). Tales from the crypt: new insights into intestinal stem cells. Nat. Rev. Gastroenterol. Hepatol. *16*, 19–34.

Gentry, L.R., Martin, T.D., Reiner, D.J., and Der, C.J. (2014). Ral small GTPase signaling and oncogenesis: More than just 15minutes of fame. Biochim. Biophys. Acta *1843*, 2976–2988.

Goh, L.K., Huang, F., Kim, W., Gygi, S., and Sorkin, A. (2010). Multiple mechanisms collectively regulate clathrin-mediated endocytosis of the epidermal growth factor receptor. J. Cell Biol. *189*, 871–883.

Golembo, M., Schweitzer, R., Freeman, M., and Shilo, B.Z. (1996). Argos transcription is induced by the Drosophila EGF receptor pathway to form an inhibitory feedback loop. Development *122*, 223 LP – 230.

González-García, A., Pritchard, C.A., Paterson, H.F., Mavria, G., Stamp, G., and Marshall, C.J. (2005). RalGDS is required for tumor formation in a model of skin carcinogenesis. Cancer Cell *7*, 219–226.

Guo, G., Gong, K., Wohlfeld, B., Hatanpaa, K.J., Zhao, D., and Habib, A.A. (2015). Ligand-Independent EGFR Signaling. Cancer Res. *75*, 3436–3441.

Hanahan, D., and Weinberg, R.A. (2011). Hallmarks of cancer: the next generation. Cell *144*, 646–674.

Hsu, T., McRackan, D., Vincent, T.S., and Gert de Couet, H. (2001). Drosophila Pin1 prolyl isomerase Dodo is a MAP kinase signal responder during oogenesis. Nat. Cell Biol. *3*, 538–543.

Hu, Y., Flockhart, I., Vinayagam, A., Bergwitz, C., Berger, B., Perrimon, N., and

Mohr, S.E. (2011). An integrative approach to ortholog prediction for disease-focused and other functional studies. BMC Bioinformatics *12*, 357.

Huang, H.-J.S., Nagane, M., Klingbeil, C.K., Lin, H., Nishikawa, R., Ji, X.-D., Huang, C.-M., Gill, G.N., Wiley, H.S., and Cavenee, W.K. (1997). The Enhanced Tumorigenic Activity of a Mutant Epidermal Growth Factor Receptor Common in Human Cancers Is Mediated by Threshold Levels of Constitutive Tyrosine Phosphorylation and Unattenuated Signaling. J. Biol. Chem. *272*, 2927–2935.

Jardé, T., Chan, W.H., Rossello, F.J., Kaur Kahlon, T., Theocharous, M., Kurian Arackal, T., Flores, T., Giraud, M., Richards, E., Chan, E., et al. (2020). Mesenchymal Niche-Derived Neuregulin-1 Drives Intestinal Stem Cell Proliferation and Regeneration of Damaged Epithelium. Cell Stem Cell.

Jiang, H., Grenley, M.O., Bravo, M.-J., Blumhagen, R.Z., and Edgar, B. a (2011). EGFR/Ras/MAPK signaling mediates adult midgut epithelial homeostasis and regeneration in Drosophila. Cell Stem Cell *8*, 84–95.

Jiang, Y., Sverdlov, M.S., Toth, P.T., Huang, L.S., Du, G., Liu, Y., Natarajan, V., and Minshall, R.D. (2016). Phosphatidic Acid Produced by RalA-activated PLD2 Stimulates Caveolae-mediated Endocytosis and Trafficking in Endothelial Cells. J. Biol. Chem. *291*, 20729–20738.

Jin, Y., Ha, N., Forés, M., Xiang, J., Gläßer, C., Maldera, J., Jiménez, G., and Edgar, B.A. (2015). EGFR/Ras Signaling Controls Drosophila Intestinal Stem Cell Proliferation via Capicua-Regulated Genes. PLOS Genet. *11*, e1005634.

Johansson, J., Naszai, M., Hodder, M.C., Pickering, K.A., Miller, B.W., Ridgway, R.A., Yu, Y., Peschard, P., Brachmann, S., Campbell, A.D., et al. (2019). RAL

GTPases Drive Intestinal Stem Cell Function and Regeneration through Internalization of WNT Signalosomes. Cell Stem Cell *24*, 592-607.e7.

Jullien-Flores, V., Mahé, Y., Mirey, G., Leprince, C., Meunier-Bisceuil, B., Sorkin, A., and Camonis, J.H. (2000). RLIP76, an effector of the GTPase Ral, interacts with the AP2 complex: involvement of the Ral pathway in receptor endocytosis. J. Cell Sci. *113 (Pt 1*, 2837–2844.

Jung, M.J., Woo, C.G., Lee, S., Chin, S., Kim, H.K., Kwak, J.J., Koh, E.S., Lee, B., Jang, K.-T., and Moon, A. (2017). Gene copy number variation and protein overexpression of EGFR and HER2 in distal extrahepatic cholangiocarcinoma. Pathology *49*, 582–588.

Kitchen, P.A., Goodlad, R.A., FitzGerald, A.J., Mandir, N., Ghatei, M.A., Bloom, S.R., Berlanga-Acosta, J., Playford, R.J., Forbes, A., and Walters, J.R.F. (2005). Intestinal Growth in Parenterally-Fed Rats Induced by the Combined Effects of Glucagon-like Peptide 2 and Epidermal Growth Factor. J. Parenter. Enter. Nutr. *29*, 248–254.

Kohlmaier, A., Fassnacht, C., Jin, Y., Reuter, H., Begum, J., Dutta, D., and Edgar, B.A. (2015). Src kinase function controls progenitor cell pools during regeneration and tumor onset in the Drosophila intestine. Oncogene *34*, 2371–2384.

Koyama, S., and Kikuchi, A. (2001). Ras interaction with Ra1GDS effector targets. pp. 127–138.

Koyama, L.A.J., Aranda-Díaz, A., Su, Y.-H., Balachandra, S., Martin, J.L., Ludington, W.B., Huang, K.C., and O'Brien, L.E. (2020). Bellymount enables longitudinal, intravital imaging of abdominal organs and the gut microbiota in adult Drosophila. PLOS Biol. *18*, e3000567.

Lanzetti, L., and Di Fiore, P.P. (2017). Behind the Scenes: Endo/Exocytosis in the Acquisition of Metastatic Traits. Cancer Res. *77*, 1813–1817.

Lesokhin, A.M., Yu, S.-Y., Katz, J., and Baker, N.E. (1999). Several Levels of EGF Receptor Signaling during Photoreceptor Specification in Wild-Type,Ellipse,and Null MutantDrosophila. Dev. Biol. *205*, 129–144.

Li, A.R., Chitale, D., Riely, G.J., Pao, W., Miller, V.A., Zakowski, M.F., Rusch, V., Kris, M.G., and Ladanyi, M. (2008). EGFR Mutations in Lung Adenocarcinomas. J. Mol. Diagnostics *10*, 242–248.

Luo, F., Brooks, D.G., Ye, H., Hamoudi, R., Poulogiannis, G., Patek, C.E., Winton, D.J., and Arends, M.J. (2009). Mutated K-ras(Asp12) promotes tumourigenesis in Apc(Min) mice more in the large than the small intestines, with synergistic effects between K-ras and Wnt pathways. Int. J. Exp. Pathol. *90*, 558–574.

Madsen, M.W., Lykkesfeldt, A.E., Laursen, I., Nielsen, K. V, and Briand, P. (1992). Altered gene expression of c-myc, epidermal growth factor receptor, transforming growth factor-alpha, and c-erb-B2 in an immortalized human breast epithelial cell line, HMT-3522, is associated with decreased growth factor requirements. Cancer Res. *52*, 1210–1217.

Mancini, M., and Yarden, Y. (2016). Mutational and network level mechanisms underlying resistance to anti-cancer kinase inhibitors. Semin. Cell Dev. Biol. *50*, 164–176.

Marchbank, T., Goodlad, R.A., Lee, C.Y., and Playford, R.J. (1995). Luminal Epidermal Growth Factor is Trophic to the Small Intestine of Parenterally Fed Rats. Clin. Sci. *89*, 117–120.

Martin, J.L., Sanders, E.N., Moreno-Roman, P., Jaramillo Koyama, L.A., Balachandra, S., Du, X., and O'Brien, L.E. (2018). Long-term live imaging of the Drosophila adult midgut reveals real-time dynamics of division, differentiation and loss. Elife *7*.

Mellman, I., and Yarden, Y. (2013). Endocytosis and Cancer. Cold Spring Harb. Perspect. Biol. *5*, a016949–a016949.

Ménard, L., Floc'h, N., Martin, M.J., and Cross, D.A. (2018). Reactivation of mutant-EGFR degradation through clathrin inhibition overcomes resistance to EGFR tyrosine kinase inhibitors. Cancer Res. canres.2195.2017.

Meng, F.W., and Biteau, B. (2015). A Sox Transcription Factor Is a Critical Regulator of Adult Stem Cell Proliferation in the Drosophila Intestine. Cell Rep. *13*, 906–914.

Micchelli, C.A., and Perrimon, N. (2006). Evidence that stem cells reside in the adult Drosophila midgut epithelium. Nature *439*, 475–479.

Mirey, G., Balakireva, M., L'Hoste, S., Rosse, C., Voegeling, S., and Camonis, J. (2003). A Ral Guanine Exchange Factor-Ral Pathway Is Conserved in Drosophila melanogaster and Sheds New Light on the Connectivity of the Ral, Ras, and Rap Pathways. Mol. Cell. Biol. *23*, 1112–1124.

Moghadam, A.R., Patrad, E., Tafsiri, E., Peng, W., Fangman, B., Pluard, T.J., Accurso, A., Salacz, M., Shah, K., Ricke, B., et al. (2017). Ral signaling pathway in health and cancer. Cancer Med. *6*, 2998–3013.

Mosesson, Y., Mills, G.B., and Yarden, Y. (2008). Derailed endocytosis: an emerging feature of cancer. Nat. Rev. Cancer *8*, 835–850.

Nászai, M., Carroll, L.R., and Cordero, J.B. (2015). Intestinal stem cell proliferation and epithelial homeostasis in the adult Drosophila midgut. Insect Biochem. Mol. Biol. *67*, 9–14.

Neel, N.F., Martin, T.D., Stratford, J.K., Zand, T.P., Reiner, D.J., and Der, C.J. (2011). The RalGEF-Ral Effector Signaling Network: The Road Less Traveled for Anti-Ras Drug Discovery. Genes Cancer *2*, 275–287.

Neyen, C., Bretscher, A.J., Binggeli, O., and Lemaitre, B. (2014). Methods to study Drosophila immunity. Methods *68*, 116–128.

Ohlstein, B., and Spradling, A. (2006). The adult Drosophila posterior midgut is maintained by pluripotent stem cells. Nature *439*, 470–474.

Parseghian, C.M., Napolitano, S., Loree, J.M., and Kopetz, S. (2019). Mechanisms of Innate and Acquired Resistance to Anti-EGFR Therapy: A Review of Current Knowledge with a Focus on Rechallenge Therapies. Clin. Cancer Res. *25*, 6899–6908.

Perochon, J., Carroll, L.R., and Cordero, J.B. (2018). Wnt Signalling in Intestinal Stem Cells: Lessons from Mice and Flies. Genes (Basel). *9*.

Powell, A.E., Wang, Y., Li, Y., Poulin, E.J., Means, A.L., Washington, M.K., Higginbotham, J.N., Juchheim, A., Prasad, N., Levy, S.E., et al. (2012). The Pan-ErbB Negative Regulator Lrig1 Is an Intestinal Stem Cell Marker that Functions as a Tumor Suppressor. Cell *149*, 146–158.

Prior, I.A., Lewis, P.D., and Mattos, C. (2012). A Comprehensive Survey of Ras Mutations in Cancer. Cancer Res. *72*, 2457–2467.

Queenan, A.M., Ghabrial, A., and Schupbach, T. (1997). Ectopic activation of torpedo/Egfr, a Drosophila receptor tyrosine kinase, dorsalizes both the eggshell and the embryo. Development *124*, 3871 LP – 3880.

Radtke, F., and Clevers, H. (2005). Self-renewal and cancer of the gut: two sides of a coin. Science *307*, 1904–1909.

Richardson, R.B., Allan, D.S., and Le, Y. (2014). Greater organ involution in highly proliferative tissues associated with the early onset and acceleration of ageing in humans. Exp. Gerontol. *55*, 80–91.

Rimawi, M.F., Shetty, P.B., Weiss, H.L., Schiff, R., Osborne, C.K., Chamness, G.C., and Elledge, R.M. (2010). Epidermal growth factor receptor expression in breast cancer association with biologic phenotype and clinical outcomes. Cancer *116*, 1234–1242.

Roberts, M., Barry, S., Woods, A., van der Sluijs, P., and Norman, J. (2001). PDGF-regulated rab4-dependent recycling of alphavbeta3 integrin from early endosomes is necessary for cell adhesion and spreading. Curr. Biol. *11*, 1392–1402.

Roberts, R.B., Min, L., Washington, M.K., Olsen, S.J., Settle, S.H., Coffey, R.J., and Threadgill, D.W. (2002). Importance of epidermal growth factor receptor signaling in establishment of adenomas and maintenance of carcinomas during intestinal tumorigenesis. Proc. Natl. Acad. Sci. U. S. A. *99*, 1521–1526.

Rodriguez-Viciana, P., and McCormick, F. (2005). RalGDS comes of age. Cancer Cell *7*, 205–206.

Sadowski, L., Pilecka, I., and Miaczynska, M. (2009). Signaling from endosomes: Location makes a difference. Exp. Cell Res. *315*, 1601–1609.

Santarius, T., Shipley, J., Brewer, D., Stratton, M.R., and Cooper, C.S. (2010). A census of amplified and overexpressed human cancer genes. Nat. Rev. Cancer *10*, 59–64.

Sato, T., Vries, R.G., Snippert, H.J., van de Wetering, M., Barker, N., Stange, D.E., van Es, J.H., Abo, A., Kujala, P., Peters, P.J., et al. (2009). Single Lgr5 stem cells build crypt-villus structures in vitro without a mesenchymal niche. Nature *459*, 262–265.

Sato, T., van Es, J.H., Snippert, H.J., Stange, D.E., Vries, R.G., van den Born, M., Barker, N., Shroyer, N.F., van de Wetering, M., and Clevers, H. (2011). Paneth cells constitute the niche for Lgr5 stem cells in intestinal crypts. Nature *469*, 415–418.

Scoville, D.H., Sato, T., He, X.C., and Li, L. (2008). Current View: Intestinal Stem Cells and Signaling. Gastroenterology *134*, 849–864.

Sell, S. (2010). On the Stem Cell Origin of Cancer. Am. J. Pathol. *176*, 2584–2594.

Sequist, L. V., Waltman, B.A., Dias-Santagata, D., Digumarthy, S., Turke, A.B., Fidias, P., Bergethon, K., Shaw, A.T., Gettinger, S., Cosper, A.K., et al. (2011). Genotypic and Histological Evolution of Lung Cancers Acquiring Resistance to EGFR Inhibitors. Sci. Transl. Med. *3*, 75ra26-75ra26.

Siegelin, M.D., and Borczuk, A.C. (2014). Epidermal growth factor receptor mutations in lung adenocarcinoma. Lab. Investig. *94*, 129–137.

Sigismund, S., Argenzio, E., Tosoni, D., Cavallaro, E., Polo, S., and Di Fiore, P.P. (2008). Clathrin-Mediated Internalization Is Essential for Sustained EGFR Signaling but Dispensable for Degradation. Dev. Cell *15*, 209–219.

Sigismund, S., Algisi, V., Nappo, G., Conte, A., Pascolutti, R., Cuomo, A., Bonaldi, T., Argenzio, E., Verhoef, L.G.G.C., Maspero, E., et al. (2013). Threshold-controlled ubiquitination of the EGFR directs receptor fate. EMBO J. *32*, 2140–2157.

Sorkin, A., and Goh, L.K. (2009). Endocytosis and intracellular trafficking of ErbBs. Exp. Cell Res. *315*, 683–696.

Sousa, L.P., Lax, I., Shen, H., Ferguson, S.M., De Camilli, P., Schlessinger, J., Camilli, P.D., and Schlessinger, J. (2012). Suppression of EGFR endocytosis by dynamin depletion reveals that EGFR signaling occurs primarily at the plasma membrane. Proc. Natl. Acad. Sci. *109*, 4419–4424.

Spano, J.-P., Lagorce, C., Atlan, D., Milano, G., Domont, J., Benamouzig, R., Attar, A., Benichou, J., Martin, A., Morere, J.-F., et al. (2005). Impact of EGFR expression on colorectal cancer patient prognosis and survival. Ann. Oncol. *16*, 102–108.

Teis, D., Taub, N., Kurzbauer, R., Hilber, D., de Araujo, M.E., Erlacher, M., Offterdinger, M., Villunger, A., Geley, S., Bohn, G., et al. (2006). p14-MP1-MEK1 signaling regulates endosomal traffic and cellular proliferation during tissue homeostasis. J. Cell Biol. *175*, 861–868.

Tomas, A., Futter, C.E., and Eden, E.R. (2014). EGF receptor trafficking: consequences for signaling and cancer. Trends Cell Biol. *24*, 26–34.

Torrance, C.J., Jackson, P.E., Montgomery, E., Kinzler, K.W., Vogelstein, B., Wissner, A., Nunes, M., Frost, P., and Discafani, C.M. (2000). Combinatorial chemoprevention of intestinal neoplasia. Nat. Med. *6*, 1024–1028.

Vieira, A. V, Lamaze, C., and Schmid, S.L. (1996). Control of EGF receptor signaling by clathrin-mediated endocytosis. Science *274*, 2086–2089.

Vigil, D., Cherfils, J., Rossman, K.L., and Der, C.J. (2010). Ras superfamily GEFs and GAPs: validated and tractable targets for cancer therapy? Nat. Rev. Cancer *10*, 842–857.

Wang, S.-H. (2000). Dual role for Drosophila epidermal growth factor receptor signaling in early wing disc development. Genes Dev. *14*, 2271–2276.

Wang, F., Weaver, V.M., Petersen, O.W., Larabell, C.A., Dedhar, S., Briand, P., Lupu, R., and Bissell, M.J. (1998). Reciprocal interactions between beta1-integrin and epidermal growth factor receptor in three-dimensional basement membrane breast cultures: a different perspective in epithelial biology. Proc. Natl. Acad. Sci. U. S. A. *95*, 14821–14826.

Wee, P., and Wang, Z. (2017). Epidermal Growth Factor Receptor Cell Proliferation Signaling Pathways. Cancers (Basel). *9*, 52.

Wong, V.W.Y., Stange, D.E., Page, M.E., Buczacki, S., Wabik, A., Itami, S., van de Wetering, M., Poulsom, R., Wright, N.A., Trotter, M.W.B., et al. (2012). Lrig1 controls intestinal stem-cell homeostasis by negative regulation of ErbB signalling. Nat. Cell Biol. *14*, 401–408.

Xu, M.J., Johnson, D.E., and Grandis, J.R. (2017). EGFR-targeted therapies in the post-genomic era. Cancer Metastasis Rev. *36*, 463–473.

Xu, N., Wang, S.Q., Tan, D., Gao, Y., Lin, G., and Xi, R. (2011). EGFR, Wingless and JAK/STAT signaling cooperatively maintain Drosophila intestinal stem cells. Dev. Biol. *354*, 31–43.

Yang, Y.-P., Ma, H., Starchenko, A., Huh, W.J., Li, W., Hickman, F.E., Zhang, Q., Franklin, J.L., Mortlock, D.P., Fuhrmann, S., et al. (2017). A Chimeric Egfr Protein

Reporter Mouse Reveals Egfr Localization and Trafficking In Vivo. Cell Rep. *19*, 1257–1267.

Yarden, Y., and Pines, G. (2012). The ERBB network: at last, cancer therapy meets systems biology. Nat. Rev. Cancer *12*, 553–563.

Yu, H.A., Tian, S.K., Drilon, A.E., Borsu, L., Riely, G.J., Arcila, M.E., and Ladanyi, M. (2015). Acquired Resistance of EGFR- Mutant Lung Cancer to a T790M-Specific EGFR Inhibitor. JAMA Oncol. *1*, 982.

von Zastrow, M. (2003). Mechanisms regulating membrane trafficking of G protein-coupled receptors in the endocytic pathway. Life Sci. *74*, 217–224.

von Zastrow, M., and Sorkin, A. (2007). Signaling on the endocytic pathway. Curr. Opin. Cell Biol. *19*, 436–445.

Zecca, M., and Struhl, G. (2002). Control of growth and patterning of the Drosophila wing imaginal disc by EGFR-mediated signaling. Development *129*, 1369–1376.

Zhang, P., Holowatyj, A.N., Roy, T., Pronovost, S.M., Marchetti, M., Liu, H., Ulrich, C.M., and Edgar, B.A. (2019). An SH3PX1-Dependent Endocytosis-Autophagy Network Restrains Intestinal Stem Cell Proliferation by Counteracting EGFR-ERK Signaling. Dev. Cell *49*, 574-589.e5.

Zhang, Y.-L., Yuan, J.-Q., Wang, K.-F., Fu, X.-H., Han, X.-R., Threapleton, D., Yang, Z.-Y., Mao, C., and Tang, J.-L. (2016). The prevalence of EGFR mutation in patients with non-small cell lung cancer: a systematic review and meta-analysis. Oncotarget *7*.

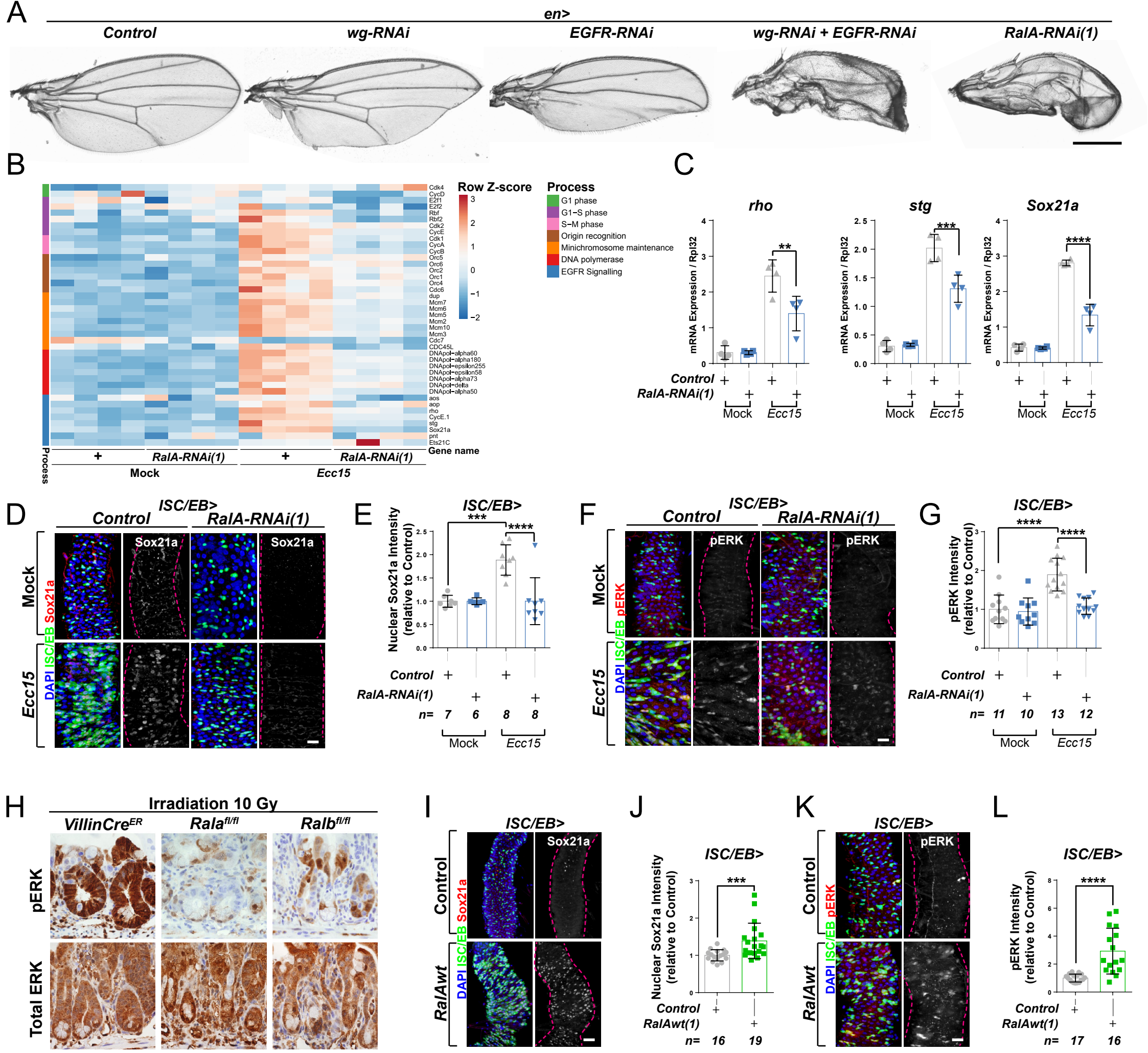
A
en>
Control
wg-RNAi
EGFR-RNAi
wg-RNAi + EGFR-RNAi
RalA-RNAi(1)
B
Row Z-score
Process
G1 phase
G1−S phase
S−M phase
Origin recognition
Minichromosome maintenance
DNA polymerase
EGFR Signalling
Gene name
RalA-RNAi(1)
Mock
Ecc15
C
rho
stg
Sox21a
mRNA Expression / Rpl32
Control
RalA-RNAi(1)
Mock
Ecc15
D
ISC/EB>
Control
RalA-RNAi(1)
Mock
Ecc15
Sox21a
DAPI ISC/EB Sox21a
E
Nuclear Sox21a Intensity (relative to Control)
n= 7 6 8 8
F
pERK
DAPI ISC/EB pERK
G
pERK Intensity (relative to Control)
n= 11 10 13 12
H
Irradiation 10 Gy
VillinCreER
Rala fl/fl
Ralb fl/fl
pERK
Total ERK
I
RalAwt
J
n= 16 19
K
L
n= 17 16

Fig 1

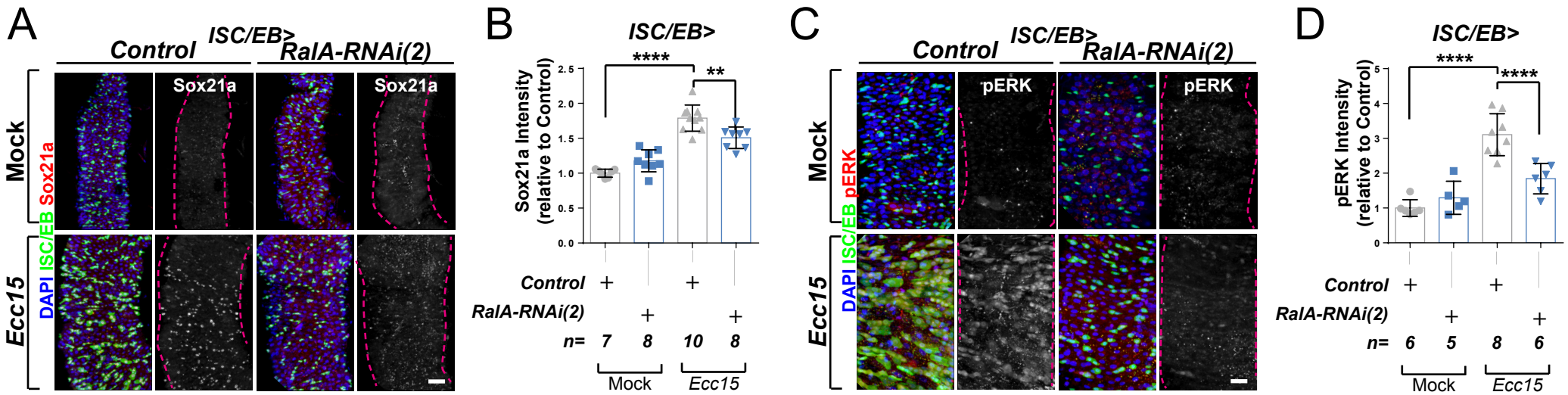

Fig 1-Supplement 1

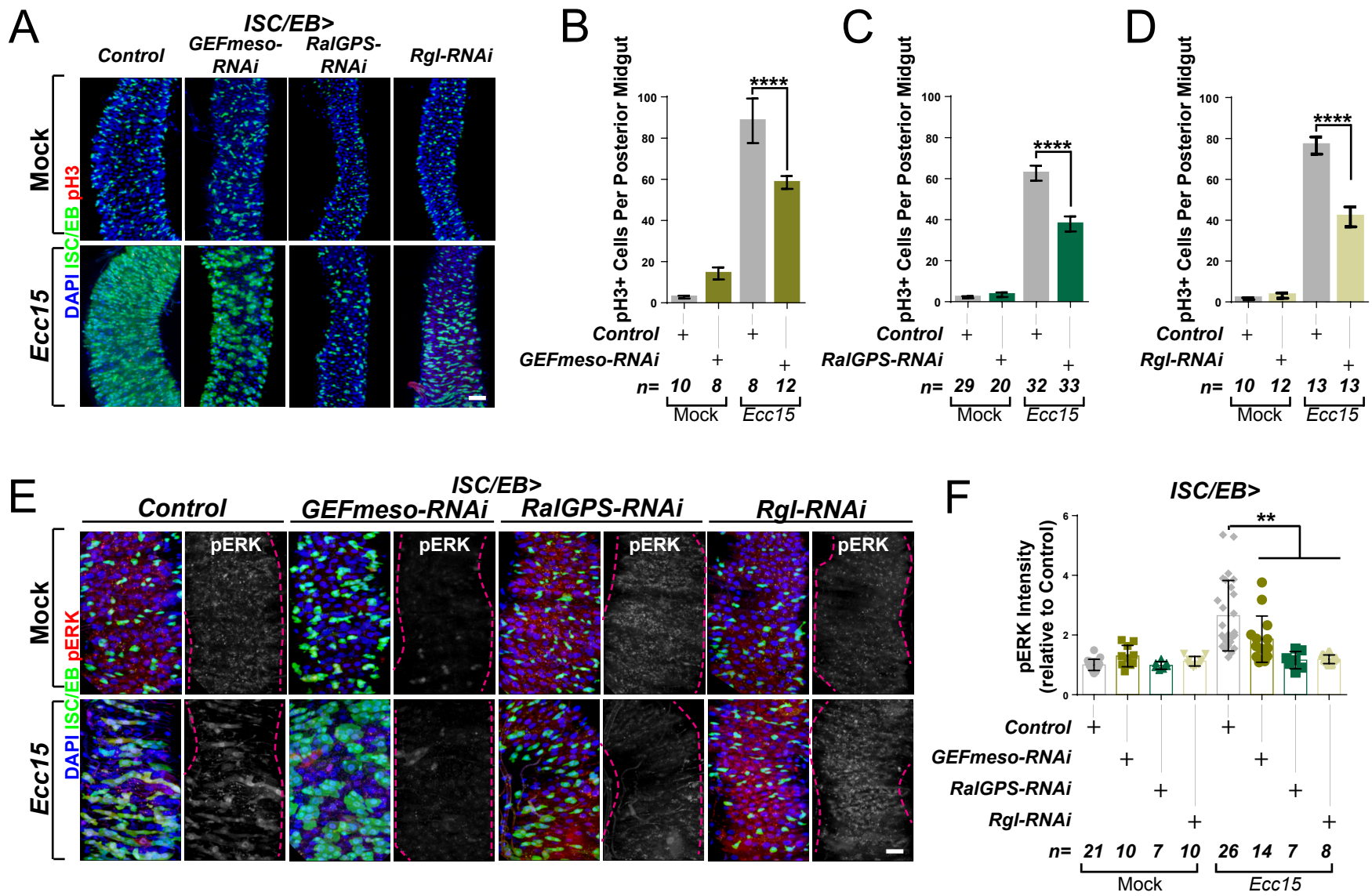
A
ISC/EB>
Control
GEFmeso-RNAi
RalGPS-RNAi
Rgl-RNAi
Mock
Ecc15
DAPI ISC/EB pH3
B
C
D
pH3+ Cells Per Posterior Midgut
****
Control
GEFmeso-RNAi
RalGPS-RNAi
Rgl-RNAi
n= 10 8 8 12
n= 29 20 32 33
n= 10 12 13 13
Mock
Ecc15
E
pERK
DAPI ISC/EB pERK
F
pERK Intensity (relative to Control)
**
n= 21 10 7 10 26 14 7 8

Fig2

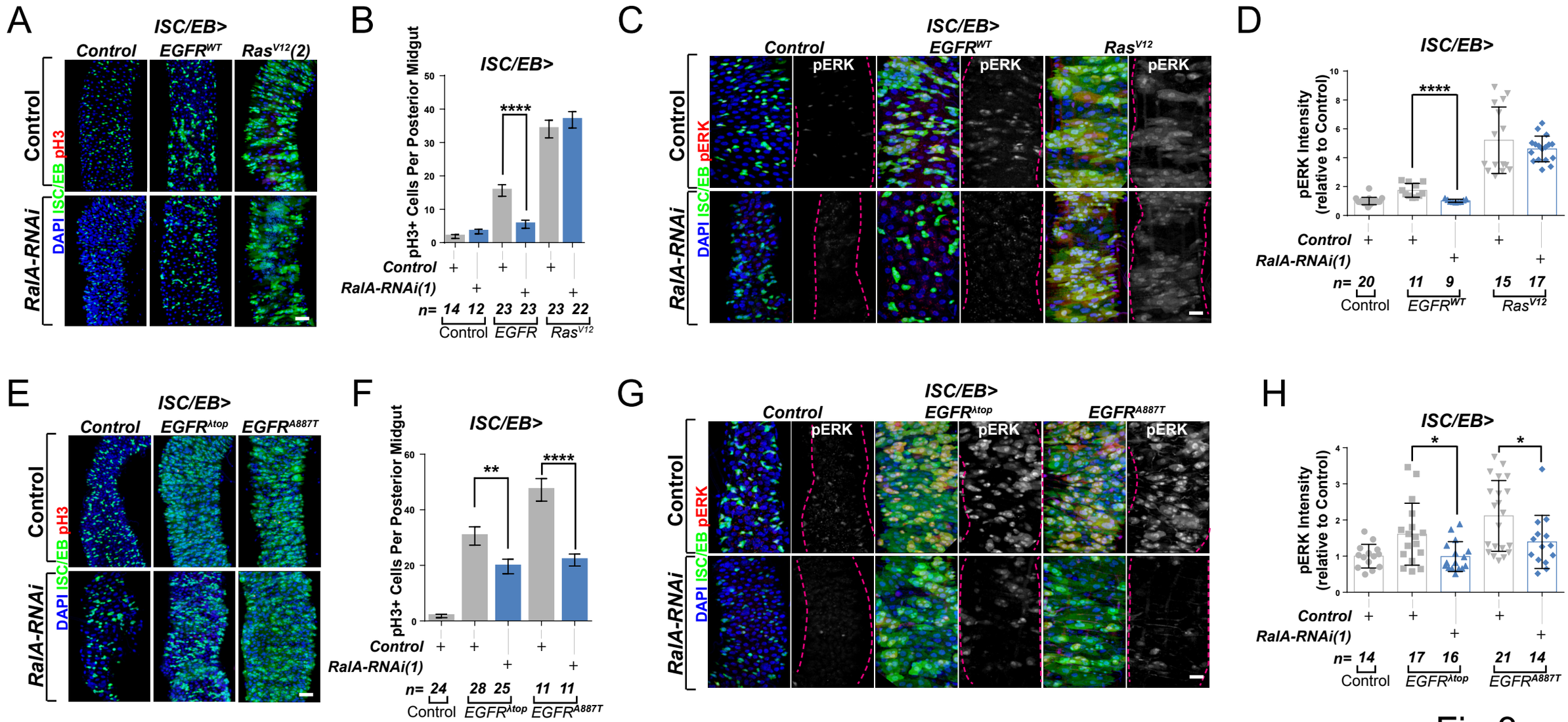
A
ISC/EB>
Control
EGFR^WT
Ras^V12(2)
Control
RalA-RNAi
DAPI ISC/EB pH3
B
ISC/EB>
pH3+ Cells Per Posterior Midgut
****
Control
RalA-RNAi(1)
n= 14 12 23 23 23 22
Control EGFR Ras^V12
C
ISC/EB>
Control
EGFR^WT
Ras^V12
pERK
Control
RalA-RNAi
DAPI ISC/EB pERK
D
ISC/EB>
pERK Intensity (relative to Control)
****
Control
RalA-RNAi(1)
n= 20 11 9 15 17
Control EGFR^WT Ras^V12
E
ISC/EB>
Control
EGFR^λtop
EGFR^A887T
Control
RalA-RNAi
DAPI ISC/EB pH3
F
ISC/EB>
pH3+ Cells Per Posterior Midgut
**
****
Control
RalA-RNAi(1)
n= 24 28 25 11 11
Control EGFR^λtop EGFR^A887T
G
ISC/EB>
Control
EGFR^λtop
EGFR^A887T
pERK
Control
RalA-RNAi
DAPI ISC/EB pERK
H
ISC/EB>
pERK Intensity (relative to Control)
*
*
Control
RalA-RNAi(1)
n= 14 17 16 21 14
Control EGFR^λtop EGFR^A887T

Fig 3

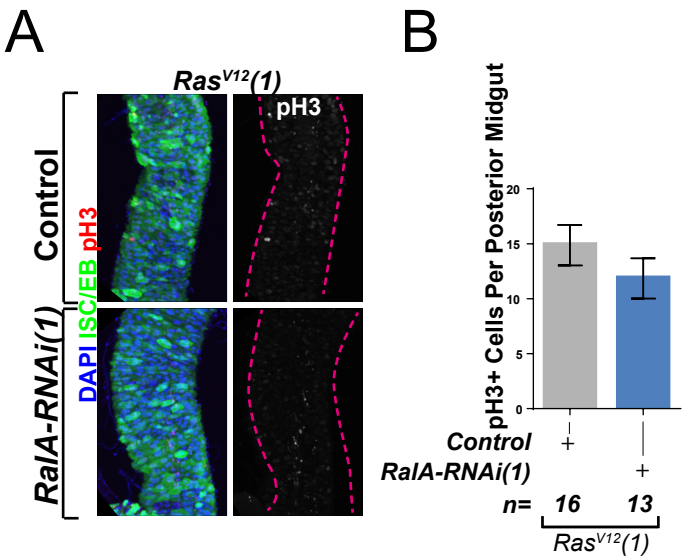

Fig 3-Supplement 1

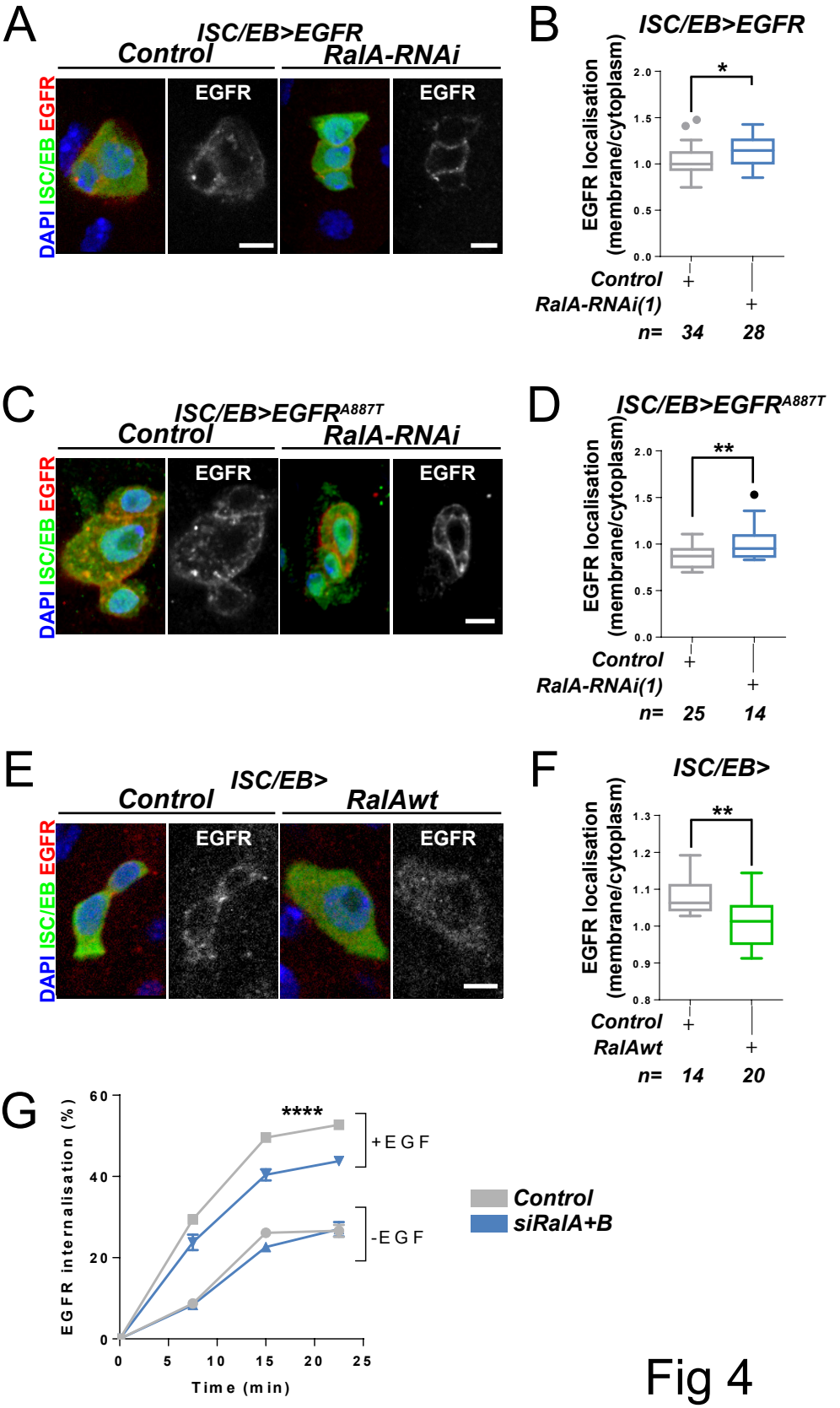
A
ISC/EB>EGFR
Control
RalA-RNAi
DAPI ISC/EB EGFR
EGFR
EGFR
B
ISC/EB>EGFR
EGFR localisation (membrane/cytoplasm)
2.0
1.5
1.0
0.5
0.0
*
Control
RalA-RNAi(1)
n= 34 28
C
ISC/EB>EGFR^A887T
Control
RalA-RNAi
DAPI ISC/EB EGFR
EGFR
EGFR
D
ISC/EB>EGFR^A887T
EGFR localisation (membrane/cytoplasm)
2.0
1.5
1.0
0.5
0.0
**
Control
RalA-RNAi(1)
n= 25 14
E
ISC/EB>
Control
RalAwt
DAPI ISC/EB EGFR
EGFR
EGFR
F
ISC/EB>
EGFR localisation (membrane/cytoplasm)
1.3
1.2
1.1
1.0
0.9
0.8
**
Control
RalAwt
n= 14 20
G
EGFR internalisation (%)
60
40
20
0
****
+EGF
-EGF
0 5 10 15 20 25
Time (min)
Control
siRalA+B

Fig 4

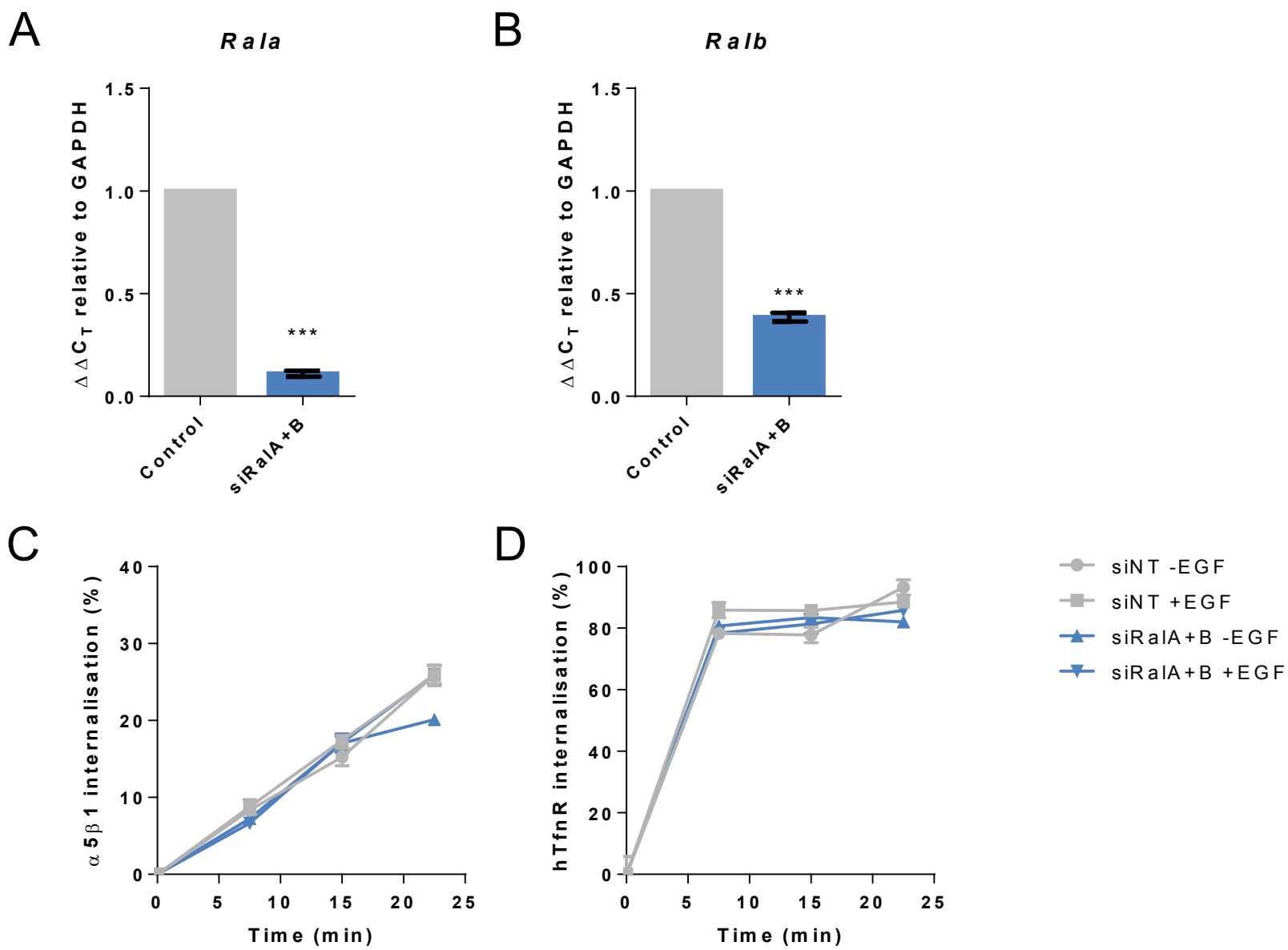

Fig 4-Supplement 1

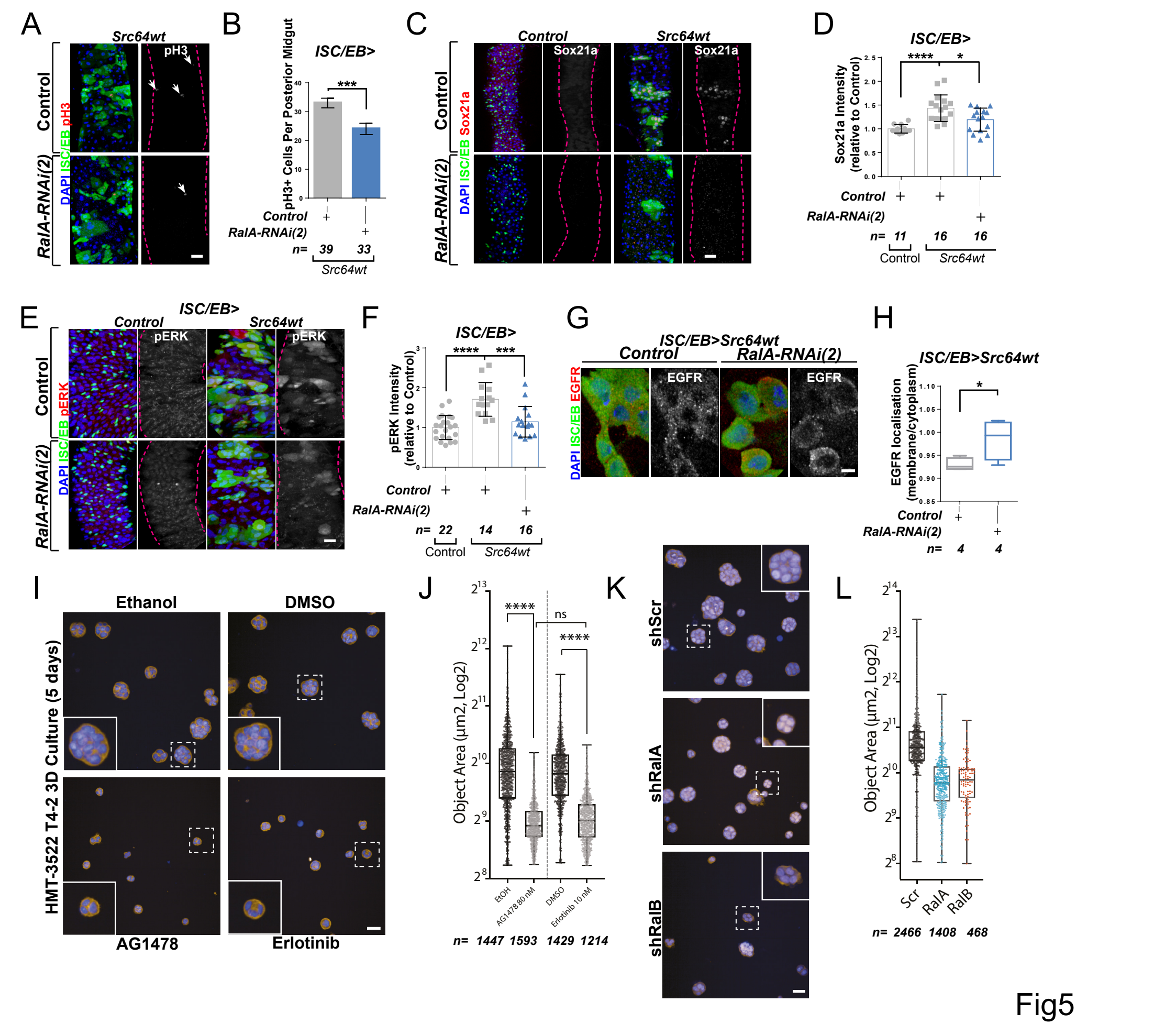
A
Src64wt
Control
RalA-RNAi(2)
DAPI ISC/EB pH3
pH3
B
ISC/EB>
pH3+ Cells Per Posterior Midgut
***
Control
RalA-RNAi(2)
n= 39 33
Src64wt
C
Control
Src64wt
Sox21a
Control
RalA-RNAi(2)
DAPI ISC/EB Sox21a
D
ISC/EB>
Sox21a Intensity (relative to Control)
****
*
Control
RalA-RNAi(2)
n= 11 16 16
Control
Src64wt
E
ISC/EB>
Control
Src64wt
pERK
Control
RalA-RNAi(2)
DAPI ISC/EB pERK
F
ISC/EB>
pERK Intensity (relative to Control)
****
***
Control
RalA-RNAi(2)
n= 22 14 16
Control
Src64wt
G
ISC/EB>Src64wt
Control
RalA-RNAi(2)
EGFR
DAPI ISC/EB EGFR
H
ISC/EB>Src64wt
EGFR localisation (membrane/cytoplasm)
*
Control
RalA-RNAi(2)
n= 4 4
I
Ethanol
DMSO
HMT-3522 T4-2 3D Culture (5 days)
AG1478
Erlotinib
J
Object Area (µm2, Log2)
****
ns
****
EtOH
AG1478 80 nM
DMSO
Erlotinib 10 nM
n= 1447 1593 1429 1214
K
shScr
shRalA
shRalB
L
Object Area (µm2, Log2)
Scr
RalA
RalB
n= 2466 1408 468

Fig5

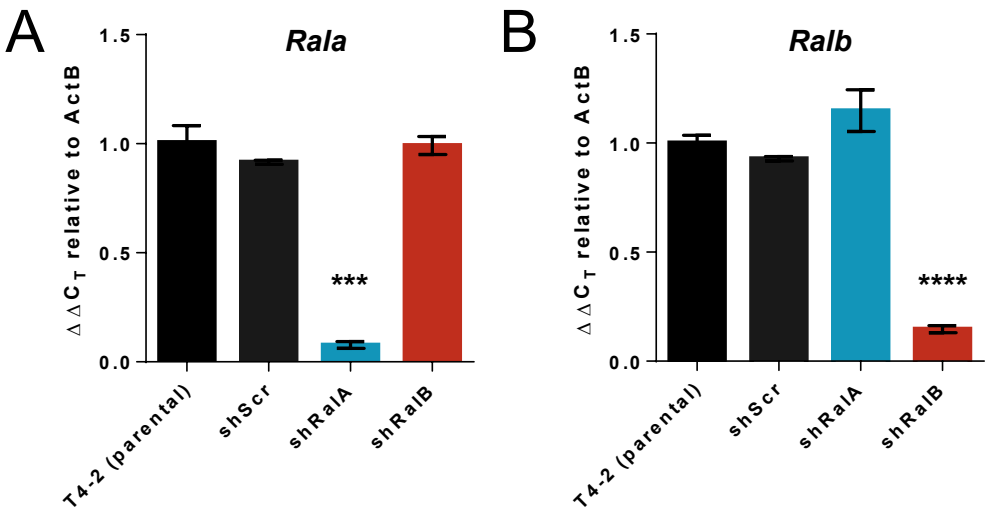

Fig 5-Supplement 1